



28 the hydrological regulation function of wetlands and reservoirs and attest that the combining of wetlands
29 with reservoir operation cannot fully eliminate the increasing future flood and drought risks. To improve
30 a river basin's resilience to the risks under future climate change, we argue that implementation of
31 wetland restoration and development of accurate forecasting systems for effective reservoir operation
32 are of great importance. Furthermore, this study demonstrated a wetland-reservoir integrated modeling
33 and assessment framework that is conducive to risk assessment of floods and hydrological droughts,
34 which can be used for other river basins in the world.

35 **Keywords:** Climate change; Hydrologic projection; Floods and droughts; Wetland hydrological
36 services; Reservoir operations; Model integration

37

38 **1. Introduction**

39 Floods and droughts have produced some of the most frequent and serious disasters in the world
40 (Hirabayashi et al., 2013; Unisdr, 2015; Diffenbaugh et al., 2015a). Globally, they account for 38% of
41 the total number of natural disasters, 45% of the total casualties, more than 84% of the total number of
42 people affected, and 30% of the total economic damage caused by all-natural disasters (Güneralp et al.,
43 2015) in the past. In the future, as climate change has been accelerating the hydrological cycle, causing
44 more frequent and stronger weather extremes, more floods and droughts have been projected to increase
45 at both regional (Hallegatte et al., 2013; Wang et al., 2021) and global scales (Jongman, 2018; Chiang
46 et al., 2021). Concurrently, the loss of disaster-related ecosystems (e.g., wetlands, forest and grassland)
47 and their services can cascade up the flood and drought risks to a great extent (Gulbin et al., 2019; Walz
48 et al., 2021). Given this, grey infrastructure such as dams, dikes, and reservoirs, which have often been
49 used to attenuate flood and drought hazards because of their rapid and visible effects, can play an
50 important role in ensuring the water security of a river basin (Casal-Campos et al., 2015; Alves et al.,
51 2019). However, relying solely on grey infrastructure to attenuate floods and droughts has some
52 inadequacies, such as large investments to build and maintain in addition to adverse effects on
53 downstream ecosystems (Maes et al., 2015; Schneider et al., 2017). In this context, Nature-based



54 solutions (NBS) for hydro-meteorological hazards mitigation are becoming increasingly popular
55 (Kumar et al., 2021), because NBS can effectively reduce or even offset the hydrological processes
56 driving floods and droughts (Nika et al., 2020), while making least disturbance to the environment as
57 well as delivering co-benefits which grey infrastructure cannot provide (Nelson et al., 2020; Anderson
58 and Renaud, 2021). Therefore, it is urgent to incorporate NBS in the current water management practices
59 to increase basin resilience to hydrological extremes under future climate change.

60 Wetlands have the potential to be used as a nature-based solution for improving water storage and
61 hence the resilience of a river basin to hydrological extremes along with grey infrastructures (Thorslund
62 et al., 2017). This is because, similar to man-made dams and reservoirs, wetlands can attenuate flow and
63 alter basin hydrological processes (Lee et al., 2018), such as floods (Wu et al., 2020a) and baseflows
64 (Evenson et al., 2015; Wu et al., 2020b). Unlike man-made grey infrastructures, wetlands are integral
65 in landscapes and they are connected laterally and vertically with the surrounding terrestrial and aquatic
66 environments through the hydrological cycling of water and waterborne substances (Ahlén et al., 2020),
67 making their water storage and cycling fundamental to estimate a watershed's water balance (Golden et
68 al., 2021; Shook et al., 2021). To understand how and to what extent wetlands can mitigate basin
69 hydrological processes, several wetland hydrological models have been developed and applied to
70 quantify hydrological functions of wetlands, particularly the mitigation services on floods and droughts.
71 For instance, Ahmed(2014) modified three parameters of NAM module in Mike11 model, i.e. the
72 maximum water content in surface storage, maximum water content in root zone storage and overland
73 flow runoff coefficient, to discern the cumulative effect of wetland loss on flood peak flow and low
74 flows. Wang et al.(2008) incorporated wetlands into SWAT model using a hydrologic equivalent
75 wetland (HEW) concept and Liu et al.(2008) developed an extension module for delineating riparian
76 wetland hydrology and embedded it into SWAT model. Since then, Evenson et al.(2016), Evenson et
77 al.(2018), Lee et al.(2018), Chen et al.(2020), Zeng et al.(2020) successively modified wetland modules
78 (isolated or riparian wetlands) and improved the applicability of SWAT model to discern hydrological
79 services of basin wetlands. Fossey et al.(2015) integrated two wetland modules (isolated and riparian
80 wetlands) into the PHYSITEL/HYDROTEL modelling platform and then investigated the impacts of



81 wetland geographic location and typology on high and low flows (Fossey et al., 2016). These wetland
82 hydrological models not only consider the general water budget of a river basin but also take into
83 account the perennial and intermittent hydrological interactions between wetlands-to-wetlands and
84 wetlands-to- surrounding landscapes. It is of both scientific and practical interest to assess the models
85 and insights arrived from them for projecting wetland capability in mitigating floods and droughts in
86 response to a changing climate.

87 Reservoirs redistribute large amounts of surface water, thus altering natural hydrological processes,
88 such as flow range, flood and drought patterns, and basin water balances (Zhao et al., 2016; Boulange
89 et al., 2021; Chen et al., 2021; Manfreda et al., 2021). So far, throughout the world, there are 57, 985
90 reservoirs registered by the International Commission on Large Dams and their total volume has been
91 reached 14, 602 km³ (Eriyagama et al., 2020). Such numerous reservoirs and their large storage capacity
92 should not be neglected in water hazard assessment and hydrological projection because of their
93 significant modification on river flow regimes. A recent study by Brunner(2021) evidenced that
94 reservoir regulation can modulate flood and drought patterns by reducing drought severity and duration,
95 as well as altering spatial flood connectedness. Boulange et al.(2021) pointed out that consideration of
96 reservoirs can significantly affect the estimation of future population exposure to flood. They called for
97 the need to integrate reservoirs in model-based impact analysis of flood exposure under climate change.
98 Dang et al. (2020a) and Yassin et al. (2019) therefore argued that failure to represent these effects could
99 limit the performance of hydrological models and suppress the applicability of such models to support
100 basin flood and drought mitigation practices. Considering the increasing number of reservoirs and the
101 requirement for more accurate management practices, there is a growing need in incorporating reservoir
102 operations into basin hydrologic simulations and predictions.

103 Despite the well-established knowledge of flow and storage regulation functions that wetlands and
104 reservoirs can provide in a river basin, most modeling assessments on floods and droughts at the basin
105 scale do not take the two components into account, or give little emphasis on the combined benefits of
106 them (Brunner et al., 2021; Golden et al., 2021). Nor are the hydrological processes associated with
107 these features implicitly including in the calibration of hydrologic models. Recent studies have



108 suggested that doing so would add significant error and larger uncertainties to simulate hydrologic
109 processes (Ward et al., 2020; Brunner et al., 2021); while integrating the wetlands or reservoir operation
110 alone into watershed-scale hydrologic models may largely minimize uncertainties (Zhao et al., 2016;
111 Dang et al., 2020; Rajib et al., 2020a; Golden et al., 2021) and improve model performance (Liu et al.,
112 2008; Fossey et al., 2015; Evenson et al., 2016; Yassin et al., 2019). Furthermore, on a global scale,
113 most river basins have wetlands and their river flow has or will experience reservoir regulation
114 (Schneider et al., 2017; Muller, 2019), which elicits two thought-provoking concerns: Can coupling
115 wetlands and reservoirs for hydrological modeling achieve a ‘1+1=2’ simulation effect to support policy
116 decisions? If yes, what will be the changes of future floods and droughts under the combined influence
117 of wetlands and reservoirs? Such concerns are important because the omission of wetlands and
118 reservoirs can cause the policy-making process to be imprecise at best and ineffective at worst. However,
119 a reservoir operation and wetland services, integrated basin-scale model rarely exist in the literature, nor
120 is it clear how floods and droughts will be changed under future climate change.

121 In a very recent study conducted in the Nenjiang River Basin, Wu et al. (2022) quantified wetland
122 flood mitigation services under future climate change and reported that future precipitation extremes
123 will cause flood risks that cannot be mitigated by wetlands. They calibrated hydrological model coupling
124 isolated wetlands and riparian wetlands but didn’t consider damming effects on flood risks and wetland
125 hydrological function. However, reservoir operation has largely altered downstream flooding processes
126 (Chen et al., 2021) and reduced flow regulation service of downstream wetlands to some extent in the
127 river basin (Wu et al., 2021). For another recent study, Rajib et al. (2020) incorporated surface
128 depression and wetland water storage into hydrologic model in the upper Mississippi River Basin and
129 found that depression-integrated model improved streamflow simulation accuracy with increasing
130 upstream abundance of depression storage. They also parameterized 15 major lakes and reservoirs using
131 their unique hydraulic design and storage-discharge information. These two studies provide insights into
132 modeling and understanding the flow and storage regulation functions provided by wetlands and
133 reservoirs, however, is it still unclear whether the combining of wetlands with reservoir operation can
134 largely reduce the risk of future floods and droughts.



135 Considering the above-introduced scientific challenges and management deficiencies, we first
136 developed a framework of hydrological modeling coupled with wetland modules and reservoir operation
137 scenarios. We applied it to a large river basin with abundant wetlands and a large reservoir, the Nenjiang
138 River Basin in northeast China, to address a central question: How will estimated future flood and
139 drought risks be changed by considering the combined effects of wetlands and reservoirs? We addressed
140 these questions by (a) assessing performance of hydrological modeling framework from the perspective
141 of streamflow processes and hydrography as well as flood and drought characteristics, (b) projecting
142 flood and drought risks in terms of their characteristic indicators using the hydrological modeling
143 framework, and (c) discussing our findings and implication for practical flood and drought risk
144 management. Our framework and results are expected to bring new insights into future floods and
145 droughts and provide a basis for decision-making to curb the growing impacts of unprecedented and
146 future extreme conditions.

147 **2. Methodology**

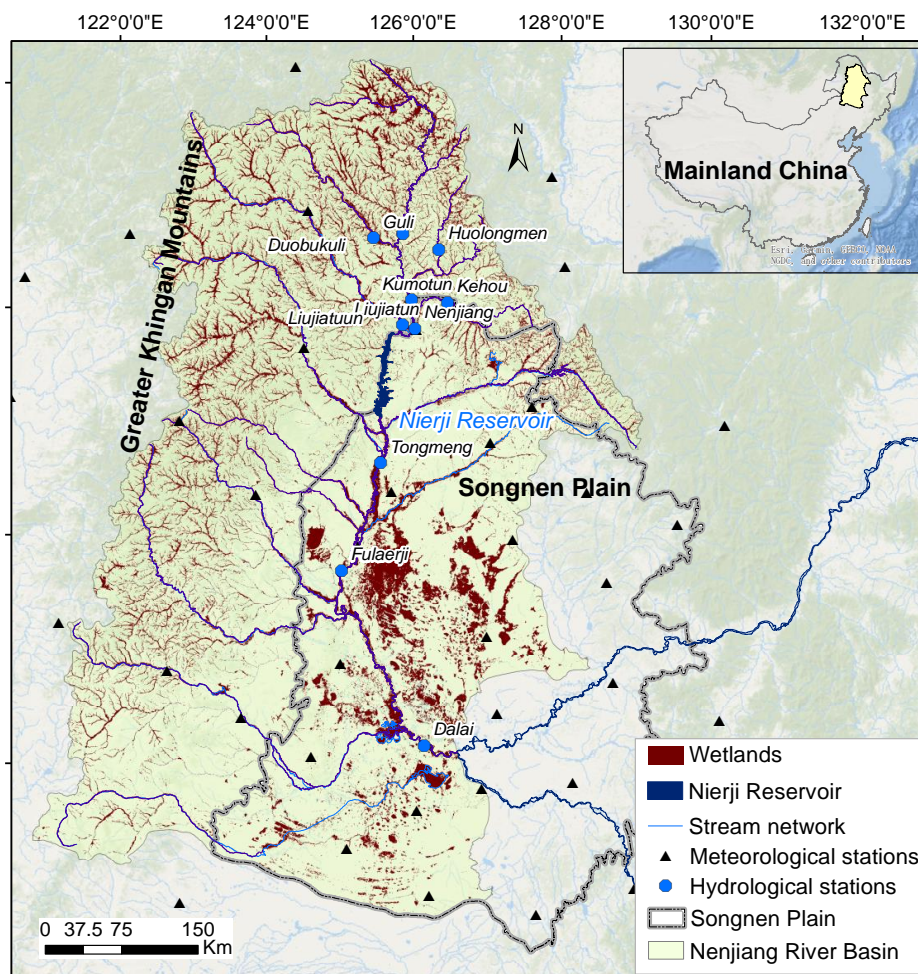
148 2.1 Study area

149 We conducted this analysis in the Nenjiang River Basin (NRB), a large river basin (291,700 km²)
150 located in the Northeast China (Fig. 1). Long-term annual average runoff depth and volume from the
151 NRB are 97.4 mm and 22.7 billion m³. The river basin is located in the middle-high latitudes and can
152 be characterized by a temperate semi-humid continental monsoon climate. Inter-annual differences in
153 temperature and precipitation are large, i.e. disparate hot and cold periods, and uneven dry and wet
154 conditions (Meng et al., 2019). The average annual temperature across the basin ranges between 2.1-
155 4.5°C. The annual total precipitation within the basin fluctuates from 323.1 to 537.6 mm. Precipitation
156 is mainly concentrated during June-September, which accounts for about 85% of the annual
157 precipitation (Li et al., 2014).

158 The NRB is one of the pivotal wetland areas in China. Many wetlands in the river basin have been
159 designated as a Ramsar Site of International Importance, including the Zalong, Xianghai, Momog and
160 Nanwen wetlands. The wetlands and their contributing drainage areas within the reaches monitored by



161 the ten hydrological stations range from 14 to 23% and from 39 to 56% respectively, demonstrating the
162 large wetland coverage of the NRB and its sub-basins (Table 1). The lower NRB is an important
163 agricultural area of the Songnun Plain, which is one of the three major plains (including the Sanjiang,
164 Songnun and Liaohe Plains) in northeast China. The Songnum Plain is also a crucial food production
165 base in China. Therefore, understanding potential floods and hydrological droughts under future climate
166 change is crucial for ensuring regional food security and ecological integrity. During the past 60 years,
167 land use and land cover types have drastically changed owing to large-scale development of intensive
168 agriculture and water resources management (Meng et al., 2019). The area of wetlands has significantly
169 decreased and their services have been degraded. For example, the area of wetlands in the NRB
170 decreased by nearly 23% from 1978 to 2000 (Chen et al., 2021), with only 16.34% remaining today
171 (Table 1). Along with the reduction in wetland area, the hydrological functions of wetlands in the NRB,
172 such as water storage, flood mitigation and baseflow support, have been considerably reduced (Wu et
173 al., 2021). These wetland services are closely related to flood and drought risks, such as the 1998 mega-
174 flood. In order to effectively deal with the risk of floods and droughts, the Nierji Reservoir was
175 constructed along the mainstream NRB (Fig. 1); it started normal operation in 2006. The Nierji
176 Reservoir is located in the upper Nenjiang River (Fig. 1). The reservoir receives inflow from an area of
177 66,382 km² and has flood control and water supply as the primary purposes and hydropower generation
178 and navigation as secondary purposes, thus playing an important role in the distribution of water
179 resources for the lower NRB.



180
181 Figure 1. Characteristics of the Nenjiang River Basin in northeast China: (a) location of stream network,
182 Nierji Reservoir, sub-basins, and hydrological and meteorological stations; elevation is also provided;
183 (b) spatial distribution of isolated (IW) and riparian (RW) wetlands and their drainage area and (c)
184 land-use types.

185
186
187
188
189



190 Table 1 The drainage area of the ten hydrological stations used in this study, area ratios of wetlands and
191 their contributing areas to the drainage area of the Nenjiang River Basin, northeast China.

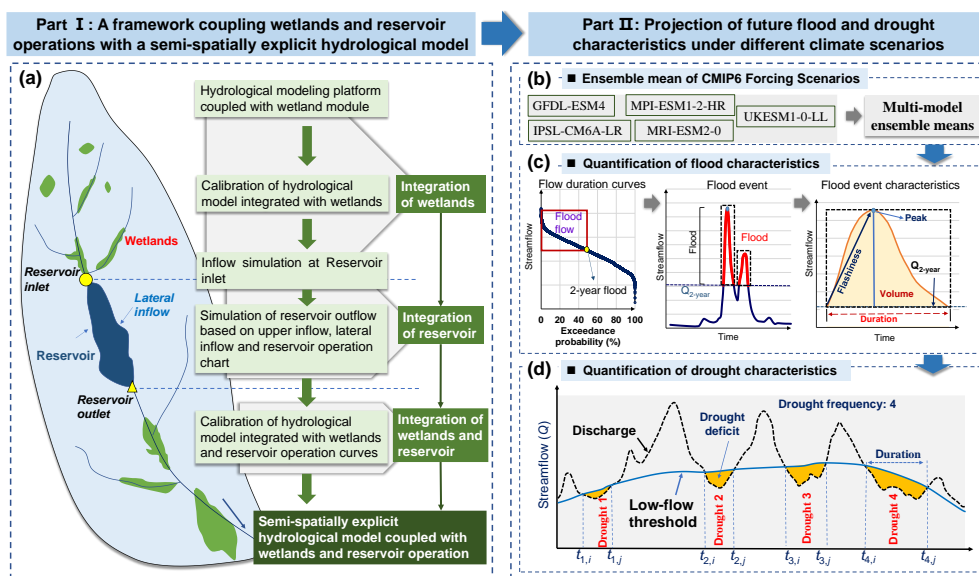
ID	River	Hydrological stations	Drainage area (km ²)	Wetland area ratio (%)	Wetland contribution area ratio (%)
1	Mainstream	Shihuiyao	17205	22.2	54.7
2	Duobukuli River	Guli	5490	16.3	57.1
3	Menlu River	Huolongmen	2151	20.8	50.7
4	Mainstream	Kumotun	32229	20.4	54.3
5	Keluo River	Kehou	7310	23.4	56.2
6	Gan River	Liujiatun	19665	13.2	49.9
7	Mainstream	Nenjiang	61249	18.3	54.1
8	Mainstream	Tongmeng	108029	13.1	47.5
9	Mainstream	Fulaerji	123911	13.7	39.0
10	Mainstream	Dalai	221715	16.3	42.4

192

193 2.2. Overview study approach

194 The methodological framework proposed in this paper includes two parts (Fig.2): (a) coupling
195 wetlands and reservoir operations with basin hydrological processes simulation, and (b) projection of
196 future flood and drought characteristics under different climate scenarios. Specifically, we first
197 developed a semi-spatially explicit hydrological model that considers wetland hydrological processes
198 and reservoir operations through coupling a distributed hydrological modeling platform with wetland
199 modules and reservoir simulation algorithms (see Part I in Fig.2 and Sect. 2.3). Then, the distributed
200 hydrological modeling platform was used to simulate streamflow driven by multi-model ensemble
201 means from the latest CMIP6 and to derive drought and flood characteristics (see Part II in Fig.2 and
202 Sect. 2.4). The flood and drought characteristics were then compared against historical periods to discern
203 how future hydrological extremes will be changed under the influence of wetlands and reservoirs.

204



205

206 Figure 2. Framework for projecting future flood and hydrological droughts based on a semi-spatially
 207 integrating wetlands and reservoir operation into a hydrological model: (a) a framework coupling
 208 wetlands and reservoir operations with a semi-spatially explicit hydrological model; (b) multi-model
 209 ensemble means from five GCM projections used for driving modeling framework; (c) methodology
 210 for determining a flood threshold, defining flood events, and extracting flood characteristics, and (d) a
 211 sequence of runs with examples of drought deficit, duration, and frequency.

212

213 2.3. Framework of hydrological modeling coupled with wetland modules and reservoir operation
 214 scenarios

215 We calibrated the model with measurements collected upstream of the reservoir inlet. The calibrated,
 216 coupled hydrologic model (i.e. hydrologic-wetland model) was then used to simulate inflow to the upper
 217 reservoir. Simultaneously, we estimated the lateral inflow into the reservoir. Based on the simulated
 218 runoff at the inlet, lateral inflow, and the schemes of reservoir operation, we estimated the reservoir
 219 outflow using the reservoir simulation algorithms. The simulated runoff simulated by hydrologic-
 220 wetland model at the reservoir outlet was replaced with the estimated reservoir outflow, thus integrating
 221 reservoir operation into the hydrological modeling (i.e. hydrologic-wetland-reservoir model). The



222 replaced runoff was used to calibrate the hydrologic-wetland-reservoir model for the lower reach of the
223 reservoir, thus integrate the downstream wetlands into the hydrologic model. Based on this framework,
224 the simulation of basin hydrological processes coupled with wetlands and reservoir operations were
225 realized.

226 2.3.1. A semi-distributed hydrological model platform coupled with wetland modules

227 We used the PHYSITEL/HYDROTEL modeling platform (Fossey et al., 2015), coupled with two
228 wetland modules, to simulate hydrological processes, assess model performance and project future flood
229 and drought conditions. This platform had been used to quantitatively evaluate the hydrological function
230 of wetlands by Fossey and Rousseau (2016), Fossey and Rousseau (2016), Blanchette et al. (2019), Wu
231 et al.(2020)a , Wu et al.(2020)b, Wu et al.(2021) and Blanchette et al.(2022). PHYSITEL is a
232 Geographic Information System based pre-processing platform for managing hydrological modeling
233 data (Rousseau et al., 2011; Noël et al., 2014). Using general basin data (a digital elevation model,
234 vectorized river network and lacustrine water bodies, and raster-based land use and soil matrix
235 distribution maps), PHYSITEL divides the basin into more detailed hydrological response units, i.e.
236 relatively homogeneous hydrological units (RHHUs) (Fortin et al., 2001). The RHHUs were defined
237 using the algorithm for delineating and extracting hillslopes proposed by Noël et al.(2014). The
238 hillslopes with same characteristics (e.g., physical geography and hydrological response) were then
239 aggregated within each RHHUs. In addition, the PHYSITEL platform distinguishes wetlands from other
240 land-use types, and then classifies both isolated and riparian wetlands based on the percentage of pixels
241 adjacent to the hydrographic network (Fossey et al., 2015). It subsequently generates data pertaining to
242 isolated and riparian wetlands and their contributing areas (CA). The PHYSITEL platform uses the
243 concept of a hydrologically equivalent wetland (HEW) proposed by Wang et al.(2008) to integrate
244 isolated wetlands (IW) and riparian wetlands (RW) at the RHHU scale. These typically large RHHUs
245 contain large wetland complexes consisting of various wetland categories such as bogs, fens, marshes,
246 and forested peatlands. After defining the hydrological and wetland parameters, PHYSITEL can directly
247 export the database as part of the input data to HYDROTEL; these data can also be used for other
248 watershed hydrological models.



249 HYDROTEL is a physically-based and semi-distributed hydrological model (Turcotte et al., 2007;
250 Bouda et al., 2012; Bouda et al., 2014) that requires wetland parameter data, land-use type maps, soil
251 texture maps, meteorological data (e.g., daily temperature and precipitation) and daily flows as input.
252 The HYDROTEL model couples the hydrological processes associated with both IWs and RWs (i.e. the
253 IWs and RWs modules) at the RHHU scale and calculates the wetland water balance with respect to the
254 surface area of the HEW, CA and RHHU. Specifically, for IWs, the hydrogeological processes are
255 integrated in the vertical water budget (Fortin et al., 2001) at the RHHU scale. For RWs, the water
256 balance is partially integrated in the vertical water budget of an RHHU and directly connected to the
257 associated river segment via the kinematic wave equation. Based on this, the IWs modules can realize
258 the vertical water balance processes of hillslope wetlands with land surface runoff processes, while the
259 RWs modules can realize the interaction of hydrological processes between RWs and river channels.
260 These representations provide a modelling approach that can simulate water balances at the wetland
261 scale while considering their interactions with the surrounding environment (contributing drainage area
262 and hydrological connectivity) (Fossey et al., 2015).

263 2.3.2. Simulation of Nierji reservoir operations

264 We used the designed operating curves of the reservoir operation chart and the ResSimOpt-Matlab
265 software package developed by Dobson et al.(2019) to simulate the operation of the Nierji Reservoir.
266 ResSimOpt-Matlab contains three algorithms for reservoir simulation. A dynamic operation schemes
267 was used in this study to achieve the simulation. Specifically, following Dobson et al.(2019) and
268 according to actual hydrological conditions, we defined two seasons: the wet season (from June to
269 September) when the risk of flooding is higher and we wanted to release the target demand and provide
270 some storage space for flood control, and the dry season when the risk of flooding is low and the main
271 objective is to sustain ecological baseflows. The required input data to the algorithm includes reservoir
272 inflow (Q_{in}), the minimum environmental flow (E_{env}), initial storage (S_o), minimum (S_{min}) and maximum
273 (S_{max}) storage, estimated evaporative losses (E_{vap}), released discharge (Q_{out}) and the simulation time-
274 step length. Based on the required data, we performed reservoir simulation by implementing the mass
275 balance equation at each simulation time step t :



$$276 \quad \begin{cases} S_{(t+1)} = S_{(t)} + Q_{in(t)} - E_{vap(t)} - Q_{out(t)} & \text{or} & S_{(t)} + Q_{in(t)} - E_{min(t)} - E_{vap(t)} \\ 0 \leq S_{(t)} \leq S_{max} \\ 0 \leq R_{(t)} \leq \min(S_{(t)} + Q_{in(t)} - E_{min(t)} - E_{vap(t)}, Q_{max}) \end{cases} \quad (1)$$

277 where S_t is the reservoir storage at time t . S_t and Q_{out} are constrained by the design specifications
278 and operation rules of a reservoir. Specifically, S_t cannot exceed the reservoir capacity S_{max} , while
279 Q_{out} is constrained by the operation schemes and capacity of the turbines Q_{max} . The excess water, if
280 any, is spilled:

$$281 \quad Q_{spill(t)} = \max(S_{(t)} + Q_{in(t)} - E_{vap(t)} - Q_{out(t)}) \quad (2)$$

282 Based on this, the dynamic Q_{out} can be represented using the equation (1) and (2).

283 We collected information on the reservoir operation including reservoir capacity, control water levels,
284 outflow, the storage-area-water level relationship, the tailwater level-discharge relationship, and the
285 maximum release, along with other data necessary to estimate the outflow. The reservoir inflow is the
286 simulated streamflow at the Nengjiang Hydrological Station, which is at the inlet of the Nierji Reservoir.
287 The minimum storage and maximum storage are 4.9 billion m^3 and 86.1 billion m^3 , respectively. Based
288 on the available data for the study area, the Karrufa method (Kharrufa, 1985) was used to estimate daily
289 evaporative losses from the reservoir. We convert days to seconds so that it would correspond to the
290 flow data. During the wet season, the actual operation schemes for the Nierji Reservoir are as follows:
291 June 1-20 is the pre-flood period with a flood limited water level of 216.0 m; June 21-August 25 is the
292 main flood period and the reasonable flood limited water level ranges from 213.4 m to 216.0 m and can
293 be gradually increased. September 6-30 is the post-flood period with a flood limited water level of 216.0
294 m. During the dry season, the environmental flow was defined as 25.3% of the daily streamflow based
295 on the designed operating curves of the reservoir operation chart.

296 2.3.3 Driving datasets, model calibration and performance assessment

297 The driving datasets used in this study include meteorological data, land-use/land-cover types, soil
298 texture, digital elevation models, drainage network, and observed discharge data. The land-use/land-
299 cover types for 2015, soil texture, digital elevation models, digital elevation models and drainage



300 network were obtained from Resource and Environment Science and Data Center
301 (<https://www.resdc.cn/>). We collected the wetland distribution maps for 2015 (extracted from National
302 wetland map in China produced by Mao et al., 2020) and overlaid it with the land-use/land-cover types.
303 Historical daily meteorological datasets including precipitation and air temperature for the period 1963-
304 2020 were obtained from 39 weather stations administered by the National Meteorological Information
305 Centre of China (<http://data.cma.cn>) and 49 weather stations in the upper NRB (Fig. 1) administered by
306 the Nenjiang Nierji Hydraulic and Hydropower Ltd. Company (<http://www.cnnej.cn>). The hydrological
307 data from ten hydrological stations were obtained from the Songliao Water Resources Commission,
308 Ministry of Water Resources (<http://www.slwr.gov.cn/>), with the time series extending from 1963 to
309 2020. Of the ten stations, seven are located upstream of the Nierji Reservoir.

310 We used observed streamflow of ten hydrological stations to calibrate the HYDROTEL model. Seven
311 hydrological stations (Shihuiyao, Guli, Huolengmen, Kumotun, Kehou, Liujiatun and Kumotun) are
312 located upstream of the Nierji Reservoir, and the rest stations (Tongmeng, Fulaerji and Dalai) are
313 installed at downstream of the reservoir. For the upstream Nierji Reservoir, we calibrated the
314 HYDROTEL model against observed streamflow of seven hydrological stations under with and without
315 wetland scenarios. Among the seven hydrological stations, the Nenjiang Station is located at the end of
316 the upstream, where the simulated streamflow was taken as the inflow of the reservoir. For the
317 downstream Nenjiang Station, we calibrated HYDROTEL model in the presence or absence of the
318 combination of wetlands and reservoir, respectively. In the case of the combination of wetland and
319 reservoir, we first simulated the operation of the Nierji Reservoir and calculated the outflow of the
320 reservoir (Sect. 2.3.2), which was used as the input streamflow for downstream model calibration. We
321 then calibrated HYDROTEL model against observed streamflow of Fulaerji and Dalai Stations under
322 with and without wetlands scenarios, respectively. Note that the without wetland scenarios are defined
323 as follows: When the wetland modules are turned off in HYDROTEL, wetland areas are not removed,
324 but they are treated as the land cover of saturated soils and thus their explicit storage properties and
325 hydrological dynamics are not accounted for in the modeling (Wu et al., 2020a). This is a basic
326 assumption that has been used in several studies using models such as SWAT (Liu et al., 2008; Wang et



327 al., 2008; Evenson et al., 2015), Mike 11 (Ahmed, 2014) and HYDROTEL (Fossey et al., 2016; Fossey
328 and Rousseau, 2016a, b; Wu et al., 2019, 2020a, 2021), to quantify the hydrologic services provided by
329 wetlands (flood mitigation, flow regulation and baseflow support etc.).

330 For all above scenarios, we calibrated the HYDROTEL model against observed streamflow at a daily
331 time step over 8 years, including a 1-year warm-up (2010.10.01-2011.09.30) and a 7-year calibration
332 (2011.10.01-2018.09.30) periods. The same model settings (i.e. key parameters, simulation periods,
333 fitting algorithm, and objective function, etc.) were used for the calibration processes under the both
334 presence and absence scenarios. Following Arsenault et al.(2018), the model was calibrated using full-
335 time observations without additional validation, as the former allows for more reliable parameters and
336 maximizes the accuracy of the model. The dynamically dimensioned search algorithm (DDS) developed
337 by Tolson and Shoemaker(2007) was used to calibrate the 13 most sensitive parameters of the model as
338 proposed by Foulon et al.(2018). Based on the maximizing of Kling-Gupta efficiency (KGE) (Gupta et
339 al., 2009), automatic calibrations using DDS were carried out utilizing 10 optimization trials. (250 sets
340 of parameters per trial). Then, the best set of parameter values out the 10 trials were selected. The KGE
341 was chosen as the objective function because previous research has shown that it can improve flow
342 variability estimates when compared to the NSE (Garcia et al., 2017; Fowler et al., 2018).

343 To determine whether coupling the wetland module and the reservoir can improve the model
344 performance, we compared (1) the efficiency of the model in simulating daily flow processes; and (2)
345 the capability of the model to simulate floods and hydrological droughts in the presence or absence of
346 the wetlands and the combination of wetlands and reservoir. Following the recommendations of N.
347 Moriasi et al.(2007) and Moriasi et al.(2015), four objective functions were selected to assess model
348 performance with regards to simulated daily flows with and without the presence of the wetland modules
349 and reservoir operation, namely the Nash-Sutcliffe efficiency (NSE) (Nash and Sutcliffe, 1970),
350 Correlation Coefficient (CC), the root-mean square error (RMSE) and the percent bias (Pbias). We used
351 multiple objective functions because it may unreliable to rely on a single objective function to determine
352 whether the model performs well (Pool et al., 2018; Fowler et al., 2018; Seibert et al., 2018). In addition,
353 we compared model performance considering daily hydrograph changes. Furthermore, flood and



354 drought features were extracted (see Sect. 2.4.2 and 2.4.3) and used to discern whether, and to what
355 extent, the coupled wetland modules and reservoir simulations could improve the model's ability to
356 simulate droughts and floods.

357 2.4. Projection of future flood and drought characteristics under different climate scenarios

358 The future simulated streamflow at the Nenjiang and Dalai hydrological stations driven by the
359 ensemble mean of bias-corrected CMIP6 Forcing Scenarios were selected to derive drought (i.e. number
360 of droughts, annual drought days, duration and deficit of each drought) and flood (i.e. peak, duration,
361 volume and flashiness) characteristics. The Nenjiang Station was chosen because it is located at the
362 outlet to (mouth of) the upper NRB and the inlet to the Nierji Reservoir, whose flood and drought
363 patterns are mainly driven by wetlands and climate change. Moreover, changes in drought and flood
364 characteristics of the Nenjiang Station are critical to the operation of the reservoir immediately lower
365 reach. The Dalai Station, located at the outlet of the entire NRB, was used as a proxy to characterize
366 future flood and drought evolution for the whole basin under the combined influence of the wetlands
367 and reservoir. Using the calibrated hydrological model that was coupled with wetlands and reservoir
368 operation, we carried out the simulation of hydrological processes for the historical period (1971-2020)
369 and under the constraints of the SSP126, SSP370 and SSP585 scenarios. We then extracted flood and
370 hydrological drought characteristic indices (see sect. 2.4.2 and 2.4.3) from the simulations to conduct a
371 comparative analysis of their temporal evolution for the near-future (2026-2050), mid-century (2051-
372 2075) and end-century (2076-2100).

373 2.4.1 Future climate change scenarios for driving hydrological modeling framework

374 In this study, we simulated potential future floods and hydrological droughts using five GCM
375 projections under three Socioeconomic Pathways (SSPs) from the latest CMIP6 (O'Neill et al., 2016).
376 Each of these specific SSPs represents a development model that includes a corresponding combination
377 of development characteristics and influences such as population growth, economic development,
378 technological progress, environmental conditions, equity principles, government management, and
379 globalization, among others; each also includes a specific description of the extent, speed and direction
380 of social development. The three SSPs that were used herein include SSP126, SSP370 and SSP585,



381 which represent potential futures characterized by green-fueled growth (van Vuuren et al., 2017), high
382 inequality between the countries (O'Neill et al., 2016) and fossil-fueled growth (Kriegler et al., 2017),
383 respectively. SSP126 is a low forcing scenario with a stable radiative forcing of approximately 2.6 W/m²
384 in 2100 (van Vuuren et al., 2017). SSP370 is a medium to high radiative forcing scenario with a stable
385 radiative forcing of approximately 7.0 W/m² in 2100 (Fujimori et al., 2017). SSP585 belongs to the high
386 forcing scenario and is the only pathway that achieves emissions as high as 8.5 W/m² by 2100 (van
387 Vuuren et al., 2017). These five GCM projections with a high resolution (0.25°) and wide application
388 (GFDL-ESM4, IPSL-CM6A-LR, MPI-ESM1-2-HR, MRI-ESM2-0, UKESM1-0-LL) were chosen to
389 provide essential output from the SSPs (Fig.2b).

390 Given the data requirements of the hydrological model, we downloaded the SSP outputs including
391 daily precipitation, maximum and minimum temperature. We then performed bias correction and spatial
392 downscaling of the SSP outputs. The bias correction of SSP outputs was carried out using the CMhyd
393 software (<https://swat.tamu.edu/software/cmhyd>), in which the widely used Delta Change method in the
394 CMhyd software was used. Delta Change bias-corrects the projected SSP outputs based on the historical
395 statistics and thus conserves the linear spatial-, temporal-, and multi-variable dependence structure in
396 the future climate (Moore et al., 2008; Bosshard et al., 2011; Maraun, 2016; Shafeeque and Luo, 2021).
397 The ANUSPLIN package developed by Hutchinson and Xu(2004) was then used to uniformly
398 downscale the output from five bias-corrected GCMs to a resolution of 1-km based on the DEM.
399 Following previous studies (Hagemann and Jacob, 2007; Zhao et al., 2021), the multi-model ensemble
400 means (M_{GCM}) of the daily precipitation, and the maximum and minimum temperature under the SSPs
401 scenarios were then obtained to diminish the uncertainties inherited in a single GCM. MEM was
402 calculated using an equally-weighted average:

$$403 \quad M_{GCM} = \frac{1}{N} \sum_{i=1}^N P_i \quad (3)$$

404 where M_{GCM} is the multi-model ensemble means, N is the number of ensemble members (5 in this study);
405 and P_i is the projected climate data of an ensemble member. In this study, the M_{GCM} of five GCMs were
406 used to drive hydrological modeling. Future changes in flood and drought characteristics from the



407 CMIP6 multi-model ensemble mean for the near-future (2026-2050), mid-century (2051-2075), and
408 end-century (2076-2100) were calculated and compared to the historical period (1970-2018). The
409 purpose of subdividing the analysis into three time periods was to compare whether, or to what extent,
410 flood and drought characteristics increase or decrease for different future time periods as compared to a
411 historical period.

412 2.4.2 Quantification of flood characteristics

413 In this study, we characterized floods in terms of four indices consisting of flood peak, flood volume,
414 duration, and flashiness (Fig. 2c). The 2-year flood streamflow was used as a threshold for defining
415 flood events, as it has been often used as a substitute of the threshold for bankfull discharge in previous
416 studies (Cheng et al., 2013; Xu et al., 2019; Wu et al., 2020). Daily streamflows that were greater than
417 the 2-year flood threshold were considered as flood flows. Flood flows occurring on multiple
418 consecutive days were considered as a single flood event. The flood indices, i.e., flood peak, volume,
419 duration, and flashiness were derived with respect to event hydrographs. Flood volume is the cumulative
420 flow from the initial to the end of a flood event with respect to the 2-year flood streamflow level, and
421 represents the flood intensity for different flood events (Wang et al., 2015). The annual total flood
422 volume is the total amount of water associated with all flood events during a water year. We calculated
423 the annual total flood volume based on flood duration and the average amount of streamflow per event
424 in a water year. Flood duration varies for different floods and is, therefore, an important characteristic
425 of a flood event. We summed the flood duration of each event in a water year to obtain the annual flood
426 days. In addition, the annual maximum peak flow was derived from the daily flows to investigate
427 changes in the characteristics of extreme floods. We extracted the 2-year flood threshold for a
428 hydrological station based on the streamflow-exceedance probability curve. Flashiness is a measure of
429 flood severity and is defined as the difference between the peak discharge and action stage discharge
430 normalized by the flooding rise time (Saharia et al., 2017).

431 2.4.3 Quantification of hydrological drought characteristics

432 We characterized hydrological drought characteristics using four indices consisting of the number of
433 droughts, annual drought days, drought duration and deficit (Fig. 2d). A threshold method was used to



434 define hydrological drought events. The threshold method is commonly used because it can
435 quantitatively determine the start and end of a hydrological drought event, which allows further
436 assessment of drought characteristics, such as frequency, duration, and intensity of a drought event
437 (Cammalleri et al., 2017). It is based on defining a flow threshold (discharge, Q , m^3/s), below which a
438 hydrological drought event is considered to occur (also known as a low flow spell). A daily variable
439 threshold, defined as an exceedance probability of the 365 daily flow duration curves was used to derive
440 drought events from daily streamflow records (Hisdal and Tallaksen, 2003; Fleig et al., 2006). For rivers
441 with perennial flow, relatively low streamflows ranging from Q_{70} to Q_{95} have been used as a reasonable
442 threshold (Zelenhasić and Salvai, 1987; Tallaksen and van Lanen, 2004). In this study, we chose the
443 90th percentile (Q_{90-n}) streamflow as the daily threshold. The Q_{90-n} of all days was determined based
444 on the observed historical daily streamflow. The daily Q_{90-n} for each hydrological station obtained in
445 this way constitutes 365 daily values, excluding the value for February 29th in leap years. The Q_{90-n}
446 values derived from the historical records were also used as the threshold for identifying droughts in
447 future climate change scenarios.

448 We analyzed the hydrological drought characteristics based on the hydrological drought threshold
449 level of Q_{90-n} . To enable the comparison across different modeling scenarios (i.e., historical scenarios
450 and future climate change scenarios), we derived drought days, deficit, duration, and number from
451 identified hydrological drought events to characterize their patterns. Drought volume deficit was
452 calculated by subtracting daily streamflow from the threshold level (Q_{90-n}) during a drought event, and
453 it presents the severity of the drought compared to the normal streamflow conditions. Drought duration
454 was the cumulative number of days during a drought event, i.e., the number of days from the beginning
455 to the end of the drought. Annual drought days were then the cumulative drought duration in a year.
456 Drought frequency is expressed by the number of drought events during a study period. Thus, the annual
457 drought frequency was defined by the cumulative number of droughts within a water year (Tallaksen
458 and Lanen, 2004). The number of droughts was the cumulative frequency of droughts within a time
459 period (e.g., a year, several years). In addition, the annual minimum flows of each water year were
460 extracted and used to determine the model's ability to simulate very low flows. The drought volume



461 deficit was calculated as:

$$462 \quad D_k = \sum_{t_i}^{t_j} (Q_{90,t} - Q_n) \cdot 60 \cdot 60 \cdot 24 \quad (4)$$

463 where D_k is the drought volume deficit (m^3) of a drought event k at a hydrological station and $t_{k,i}$ and $t_{k,j}$
464 are the initial and final time steps of the run, respectively. Q_n is the daily streamflow of n day of the year
465 (1-365). The corresponding drought duration is computed as $t_j - t_i + 1$.

466 For hydrological drought events that occur relatively close in time, the inter-event time method
467 introduced by Zelenhasić and Salvai(1987) was used to separate events. This method defines a minimum
468 gap period, t_c , and assumes that if the inter-event time $(t_j - t_i + 1) < t_c$, then the consecutive events are
469 interdependent and merged. In this case, the total drought deficit volume is the sum of the individual
470 deficit values, and the event duration is the so-called real drought duration (sum of the single event
471 duration, excluding excess periods). For this study, t_c was set equal to 7 days as recommended by
472 Cammalleri et al.(2017).

473

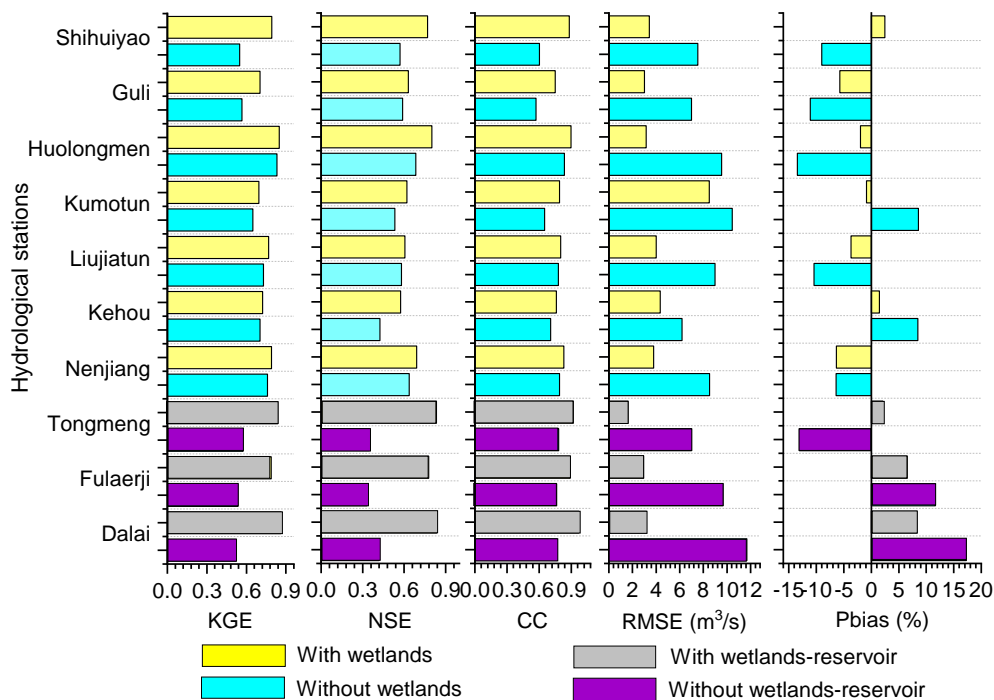
474 3. Results

475 3.1 Model performance on daily streamflow and hydrography

476 Fig. 3 depicts model performances for calibration results in the presence or absence of the wetlands
477 and the combination of wetlands and reservoir at the ten hydrological stations in the NRB. In the case
478 of whether the wetlands were present or absent, the simulated daily streamflow results all achieved the
479 acceptable performance criteria ($\text{NSE} > 0.5$ and $\text{Pbias} \leq \pm 15\%$) suggested by Moriasi(2007) and Moriasi
480 et al.(2015) at the Shihuiyao, Guli, Huolengmen, Kumotun, Kehou, Liujiatun and Kumotun stations.
481 However, compared with the calibrated results of the model without wetlands, the simulation efficiency
482 under with wetland scenario improved to varying degrees. Specifically, the relative improvement (i.e.,
483 the relative change) of KGE values at Shihuiyao, Guli, Huolengmen, Kumotun, Kehou, Liujiatun,
484 Kumotun, Tongmeng, Fulaerji and Dalai were 44%, 24%, 2%, 6%, 5%, 3%, 4%, 46%, 47% and 67%,
485 respectively. In addition, the NSE and CC values were generally larger in the presence of wetlands than
486 those in the absence of wetlands, and the RMSE and Pbias values are generally smaller than those in



487 the absence of wetlands, showing that integrating wetlands into the hydrological model can slightly
 488 improve the model calibration results.



489

490 Figure 3. Model performances for calibration results for the with/without wetlands and reservoir

491 scenarios at the ten hydrological stations in the Nenjiang River Basin. The KGE, NSE, CC, KGE,

492 RMSE and Pbias refer to Kling-Gupta efficiency, Nash-Sutcliffe efficiency, Correlation Coefficient,

493 Root Mean Square Error, and the percentage bias, respectively.

494

495 For the lower reaches of Nierji Reservoir (i.e., the Tongmeng, Fulaerji and Dalai stations, representing

496 inclusion of the wetlands and the reservoir operation into hydrological modeling), the NSE and CC

497 values were greatly higher and RMSE and Pbias values were substantially lower when the wetlands and

498 reservoir were considered, in comparison to the case without wetlands-reservoir (Fig. 3). Specially, in

499 the scenario without wetlands-reservoir, the simulated daily streamflow results failed the acceptable

500 performance criteria (NSE > 0.5 and Pbias ≤ ±15% as suggested by Moriasi (2007) and Moriasi et al.

501 (2015). In addition, the simulated daily streamflow in the no-wetland and no wetlands-reservoir



502 scenarios both overestimated the high flows, especially those during the flood periods; during the low
503 flow periods, the low flows were underestimated (Please refer to Fig. A1 in Supplementary materials).
504 Further, the simulated hydrographs under the wetland and wetlands-reservoir scenario were in much
505 better agreement with the hydrographs of observed streamflow, especially during floods and the low-
506 flow period (Please refer to Fig. A2 in Supplementary materials). These results indicate that inclusion
507 of the wetlands and the operation of reservoirs can greatly improve model capacity to replicate basic
508 hydrograph characteristics and capture hydrological extremes (e.g., high and low flows).

509 3.2 Model capacity to replicate flood and drought characteristics

510 The simulated annual minimum streamflow for the wetlands/wetlands-reservoir scenarios were, in
511 general, slightly overestimated or approximately equivalent to the observations compared to the
512 scenarios that did not include the wetlands/wetlands-reservoir (Please refer to Fig. A3 in Supplementary
513 materials). However, the simulation results without wetlands clearly underestimated minimum
514 streamflow, distinctly overestimated annual drought days and drought deficit compared to the
515 simulation results for the scenario with wetlands at the ten hydrological stations. In addition, the
516 simulated annual maximum peak flow, flood days and volume under the with/without wetland scenarios
517 are, in general, approximately comparable to observations at the Guli, Kumotun, Kehou, Liujiatun and
518 Nenjiang hydrological stations (Please refer to Fig. A4 in Supplementary materials). Specifically, for
519 the upstream Nierji Reservoir, it is apparent that if wetlands are not considered, the number of annual
520 flood days will be overestimated, whereas flood volume will be substantially underestimate at the
521 Huoloengmen Station. For the lower reach of Nierji Reservoir, lack of integrating the wetlands and
522 reservoir into the simulation can lead to a notable underestimation of annual flood days, and a substantial
523 overestimation of the annual maximum peak flow and flood volume. These results demonstrate that
524 integrating wetlands and the combination of wetlands and the reservoir into the model can help improve
525 model performance with regards to flow during the calibration process, and enhances the model's
526 capability of depicting streamflow processes as well as capturing flood and drought characteristics.

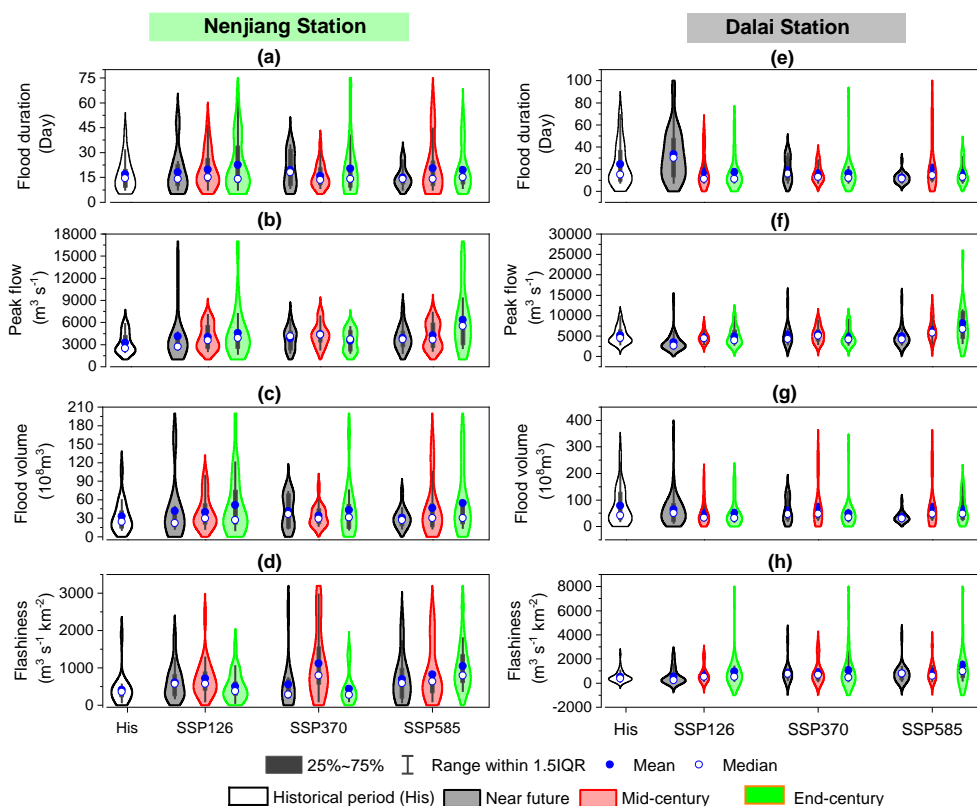
527



528 3.3 Projection of future floods

529 A comparison between historical and projected flood characteristics at the Nenjiang Station
530 (representing inclusion of wetlands into hydrological modeling) shows an overall increase in flood risks
531 in the upper NRB. The flood duration, peak flow, volume and flashiness generally exhibit larger
532 fluctuations in most of the scenarios (different SSPs and three periods as shown in Fig.4a-d, Fig.5a-d
533 and Table A1). In addition, the averaged increase in flood duration, peak flow, volume and flashiness
534 ranges from 0.9 to 1.2%, from 16 to 33%, from 8 to 111% and from 26 to 55%, respectively (Fig.5).
535 Specifically, the extreme values of flood duration are much larger during the near future and end-century
536 under the SSP126 scenario, the end-century under the SSP370 scenario and the mid- and end-century
537 under the SSP585 scenario. Apart from a slight decrease during the near future and mid-century under
538 the SSP585 scenario, peak flow will increase through time in the SSP126, SSP370 and SSP585 scenarios
539 (Fig. 4b). Simultaneously, the flood volume will experience the greatest increase of 68% during the near
540 future under the SSP585 scenario, followed by a 22% increase during the mid-century under the SSP126
541 scenario. In terms of flashiness, the floods will be more severe under the constrains inherent in the
542 SSP126 and SSP585 scenarios and less severe given the conditions in the SSP370 scenario, as compared
543 to the historical period (Fig. 4d).

544 It should be noted that the flood duration, peak flow, volume and flashiness can decrease in the future,
545 as compared to the historical period (Fig.5). For example, flood duration will slightly decrease during
546 the near future and end-century under the SSP126 scenario, largely decrease during the near future under
547 the SSP585 scenario, respectively. Under the SSP585 scenario, the flood peak flow will experience a
548 decrease with the percentage change values of 15% during the mid-century and the volume will reduce
549 26% during near future. In addition, future flood flashiness will be reduced by 49% and 28% in the near
550 future and the end-century under the SSP370 scenario respectively, and by 21% at mid-century under
551 the SSP585 scenario.



552

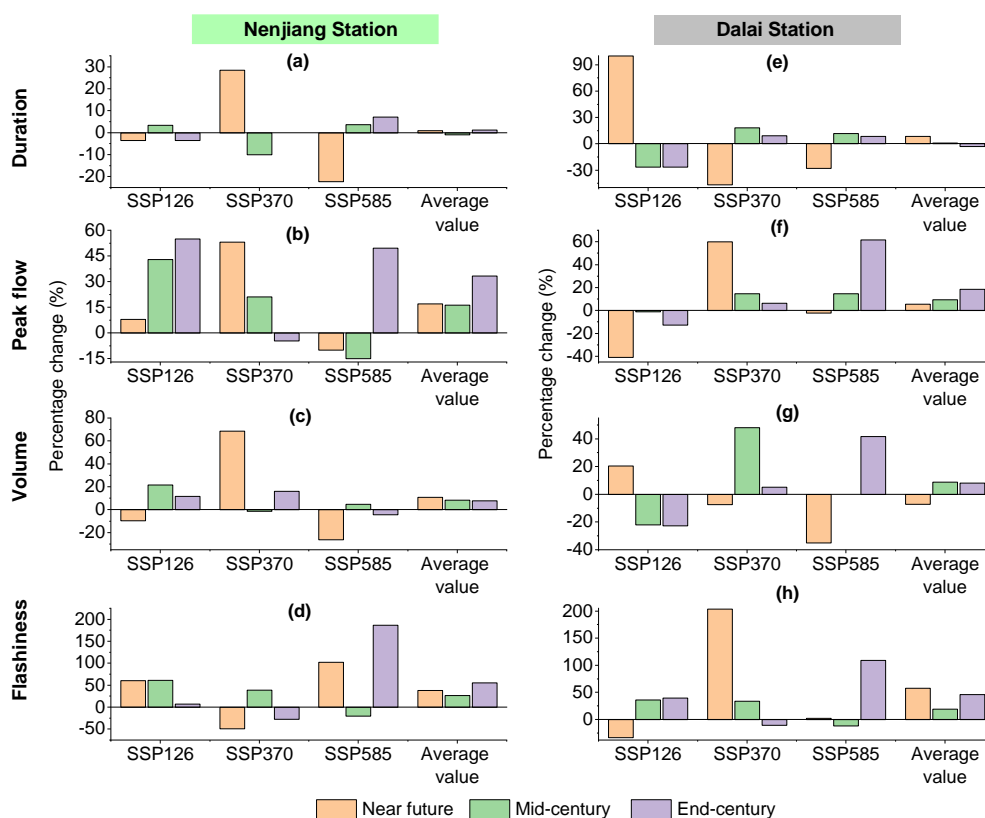
553 Figure 4. Historical and projected flood duration, peak flow, volume and flashiness at the Nenjiang (the
 554 left column) and Dalai (the right column) Station. The historical period refers to 1971-2020 and the
 555 near-future, mid-century and end-century refer to the 2026-2050, 2051-2075 and 2076-2100 under the
 556 Socioeconomic Pathways (SSP) 126, SSP370 and SSP585 scenarios. Note that the wider the violin plot,
 557 the higher the density.

558

559 The changes in the historical and future flood duration, peak flow, volume and flashiness at the Dalai
 560 Station (representing inclusion of downstream wetlands and reservoir operation into hydrological
 561 modeling) is shown in Fig.4 e-h and Fig.5 e-h. Similar to the Nenjiang station, the flood duration, peak
 562 flow, volume and flashiness at the Dalai station also exhibit divergent change trends across different
 563 SSPs and three periods, as compared to the historical periods. Flood duration is projected to increase
 564 largely in the near-future period for the SSP126 scenario, both in the mid-century and end-century for



565 the SSP370 scenario. The peak flow will broadly decrease for the SSP126 scenario, increase for the
 566 SSP370 and 585 scenarios. The relative change of flood volume will be varying considerably and
 567 contrarily from near-future to the end-century. Flood volume will decrease in the near-future and
 568 decrease in the end-century for both scenarios of SSP126 and SSP370. Flashiness will be reduced in the
 569 near-century and will increase in the mid-century and end-century for the SSP126 scenario. For the
 570 SSP370 scenario, flashiness will increase substantially with percentage changes of 204% in the near-
 571 future, Moreover, for the SSP585 scenario, flashiness will experience a considerable increase of
 572 flashiness with percentage changes of 109% in the end-century respectively. In terms of the averaged
 573 percentage change values, the peak flow and flood flashiness will overall increase; the flood volume
 574 will reduce in the near future and rise in the mid-century and end-century; and flood duration will
 575 experience a slight increase to a minor decrease.
 576



577

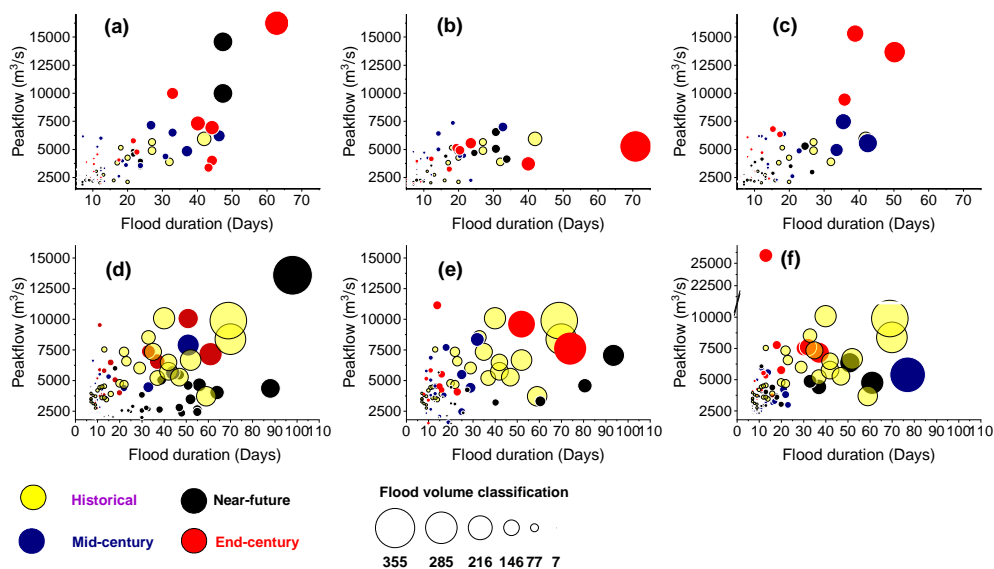


578 Figure 5. Projected percentage changes (relative to historical period during 1971-2020) in flood duration,
579 peak flow, volume and flashiness at the Nenjiang (the left column) and Dalai (the right column) Station. The
580 near-future, mid-century and end-century refer to the 2026-2050, 2051-2075 and 2076-2100 under the
581 Socioeconomic Pathways (SSP) 126, SSP370 and SSP585 scenarios. The average values were calculated
582 based on the projected percentage changes in the three SSP scenarios.

583

584 To further investigate flood risks in the NRB under future climate change, the flood duration-peak
585 flow-flow volume relationships at the Nenjiang and Dalai stations for the SSPs were compared to those
586 of the historical period and analyzed (Fig. 6a-c). Compared with historical flood risk, extreme flood
587 events with longer and larger volumes will occur more frequently at the Nenjiang Station for the SSP126
588 and SSP585 scenarios (Fig. 6a and 6c). It is noteworthy that the flood peak-volume-duration
589 relationships between the historical period and SSP370 scenario are approximate equal, with the
590 exception that longer duration and larger volume floods will occur during the end-century period (Fig.
591 6b). In addition, extreme flood events will occur mainly in the near-future for the SSP126 scenario and
592 during the medium and far future periods for the SSP585 scenario. Moreover, for the SSP370 and
593 SSP585 scenarios, floods will become shorter in duration, and possess a lower peak flow and flood
594 volume in the near-future. Thus, the upper NRB will experience more severe flood events to a large
595 extent under most future climate change.

596



597

598 Figure 6. Historical and projected flood duration-peak flow-volume relationships at the Nenjiang (the
 599 first row) and Dalai (the second row) Station. The historical period refers to 1971-2020 and the near-
 600 future, mid-century and end-century refer to the 2026-2050, 2051-2075 and 2076-2100 under the
 601 Socioeconomic Pathways (SSP) 126, SSP370 and SSP585 scenarios.

602

603 The duration-peak flow-volume relationships of extreme flood events under future climate change
 604 scenarios are closer to those of the historical period at the Dalai Station than at the Nenjiang Station
 605 (Fig. 6e-f). For the three future SSPs, the flood events with longer duration, higher peak flows or larger
 606 volume than the historical period will occurred infrequently, and the duration, flood volume and peak
 607 flow of the other shorter and lower magnitude flood events will generally be attenuated. However, very
 608 extreme flood events are projected to occur in the near-future under the conditions of scenario SSP126.
 609 Likewise, future climate change under the SSP370 scenario and 585 scenarios are projected to result in
 610 longer flood events in the near-future and mid-century, respectively. Therefore, the future flood risk can
 611 be effectively attenuated to a great extent by the combined influence of wetlands and reservoir. However,
 612 the fact that extreme flood events that will still occur in the future.

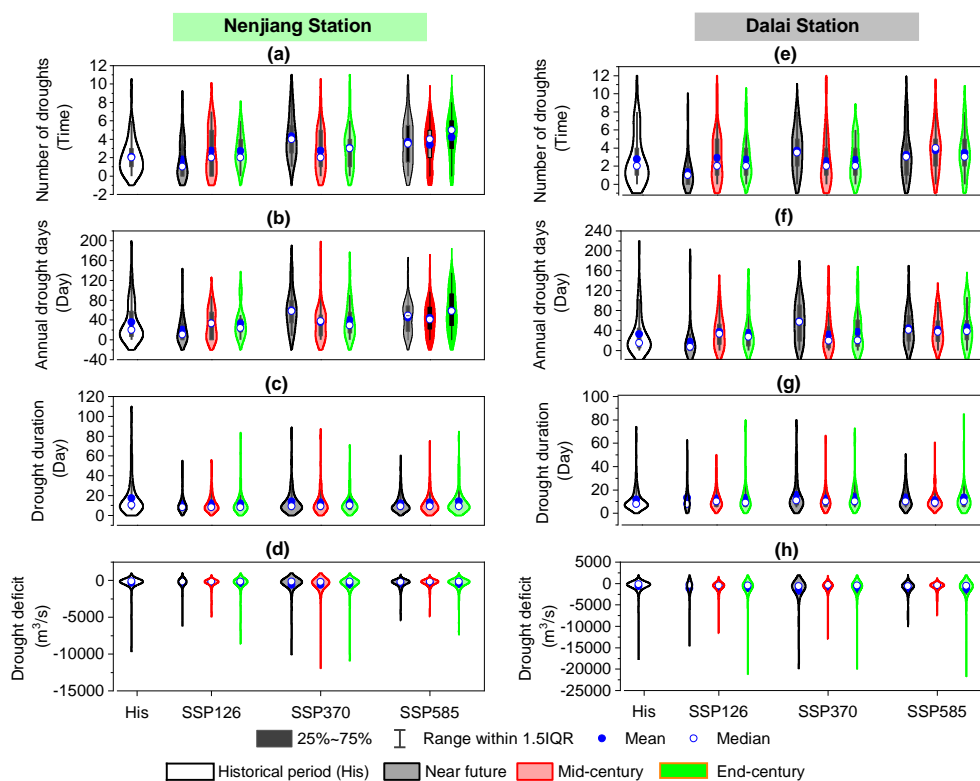


613 3.4. Prediction of future hydrological droughts

614 The comparison between historical and projected hydrological drought indices shows that the risks
615 of hydrological droughts will be increase to some extent under future climate change for both Nenjiang
616 and Dalai stations. Specifically, in addition to a reduction in the number of droughts and annual drought
617 days in the near future for the SSP126 scenario, the number of droughts, annual drought days and
618 drought deficit will overall increase in other periods for three scenarios (Fig. 7 and Fig. 8; Table A2). It
619 is clearly that the number of droughts will equivalent to the historical period in the mid-century and end-
620 century for the SSP126 scenario and in the mid-century for the SSP585 scenario. For all other scenarios,
621 the number of droughts will increase. In terms of the mean percentage change values, there is a general
622 trend towards an increase in the number of droughts and annual drought days, which indicate that future
623 drought events will be more frequent and there will be more days per year affected by drought (Fig. 8).
624 The predicted extreme values show that the future duration of drought at Nengjiang station may shorter
625 than the historical period, but the degree of shorting presented in different SSP scenarios varies. For the
626 Dalai station, the longest drought durations would all exceed historical extremes in the end-century for
627 the ssp126 and SSP585 scenario, and in the near future for the SSP370 scenario. The percentage change
628 values display that drought duration will be reduced at the Nenjiang station and will be extended at the
629 Dalai station for all the SSP scenarios. Drought deficit at the Dalai station will increase by 39%, 36%
630 and 36% and in the near future, mid-century and end-century. For the Dalai station, drought deficit will
631 increase further in the three periods with 39%, 36% and 36%, respectively.

632 A comparison of the percentage change values between the Nengjiang and Dalai stations shows that,
633 apart from a reduction of the number of drought events, the risk of drought to be experienced at Dalai
634 is considerably stronger than at Nengjiang. Specifically, the percentage change in the annual drought
635 days, drought duration and deficit will increase from 85-97% to 89-134%, from -17- -17% to 21%, and
636 from 36-39% to 171-247%, respectively.

637

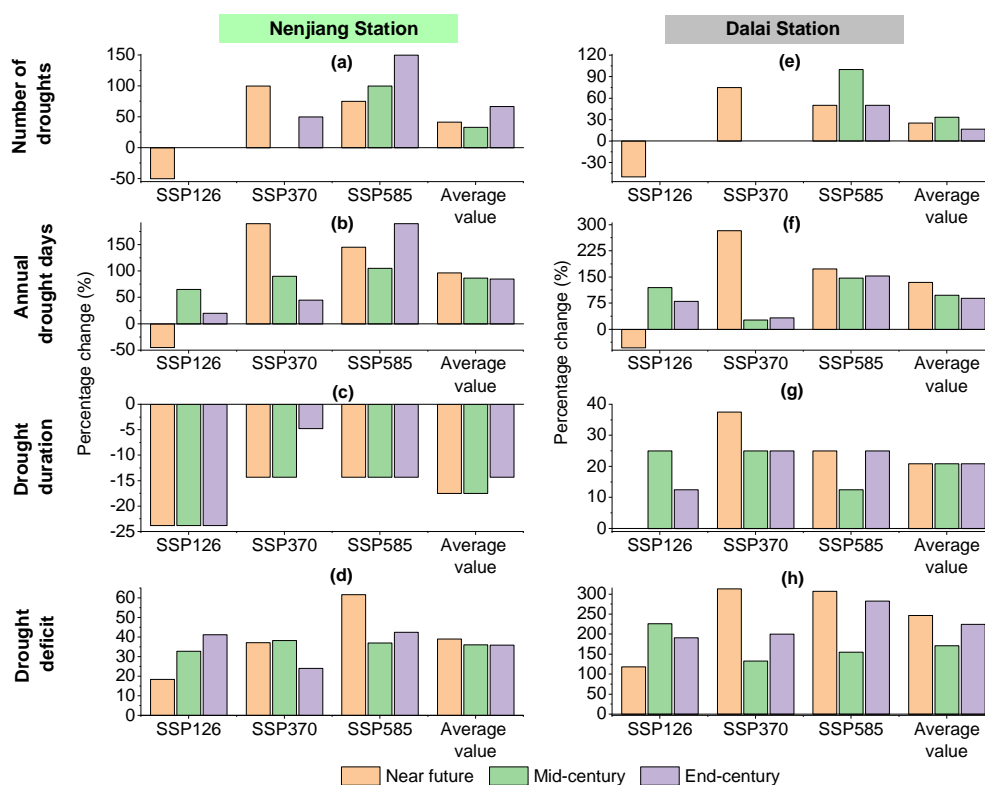


638

639 Figure 7. Historical and projected hydrological drought characteristics (the number of droughts, annual
 640 drought days, duration, and deficit) at the Nenjiang (the left column) and Dalai (the right column) Station.

641 The historical period refers to 1971-2020 and the near-future, mid-century and end-century refer to the 2026-
 642 2050, 2051-2075 and 2076-2100 under the Socioeconomic Pathways (SSP) 126, SSP370 and SSP585
 643 scenarios. Note that the wider the violin plot, the higher the density.

644



645

646 Figure 8. Projected percentage changes (relative to historical period during 1971-2020) in hydrological
 647 drought characteristics at the Nenjiang (the left column) and Dalai (the right column) Station. The near-future,
 648 mid-century and end-century refer to the 2026-2050, 2051-2075 and 2076-2100 under the Socioeconomic
 649 Pathways (SSP) 126, SSP370 and SSP585 scenarios. The average values were calculated based on the
 650 projected percentage changes in the three SSP scenarios.

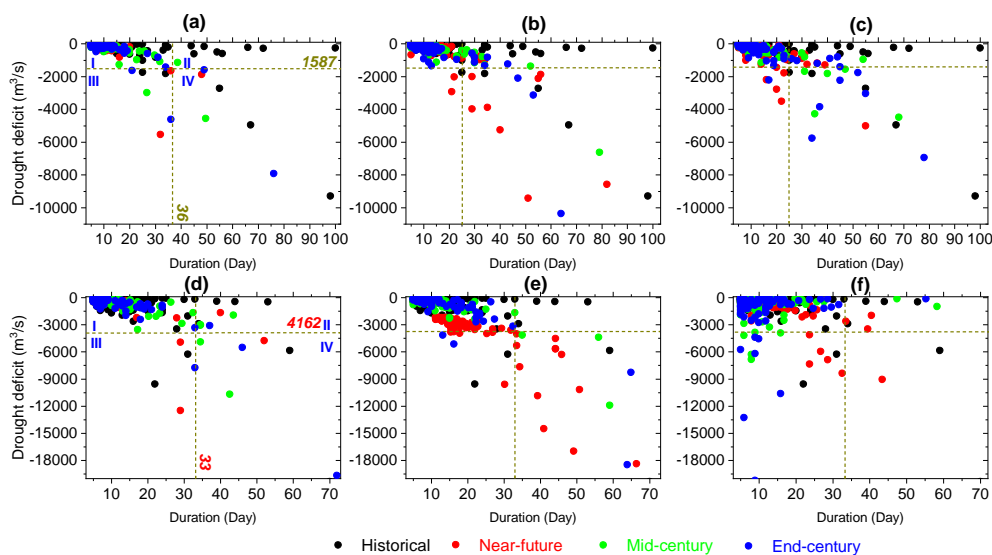
651

652 To further analyze the temporal evolution of droughts in the Nenjiang River Basin under future
 653 climate change, drought events were classified into four types in terms of duration and deficit, i.e., short-
 654 term light droughts, long-term light droughts, short-term severe droughts, and long-term severe droughts
 655 (see Fig. 9 for details). This four-part classification was then used to compare and analyze the changes
 656 in the temporal characteristics of drought events under the different SSP scenarios. Similar to the
 657 drought characteristics during the historic historical period, the majority of drought events for the



658 SSP126, SSP370 and SSP585 scenarios are short-term light droughts (Fig. 9a, 9b and 9c), i.e., the upper
659 NRB will still be dominated by short-term light droughts under future climate change. However, these
660 droughts will be slightly aggravated and marginally longer. In addition, long-term light droughts will
661 occur rarely under the conditions inherent in scenarios SSP126 and SSP370, and occur relative
662 frequently in the SSP585 scenario. However, compared with the historical period, the overall number
663 of long-term light droughts will largely decrease, but the deficit will increase slightly under future
664 climate change. In addition, short-term severe droughts will increase substantially, along with their
665 deficit. The number of long-term severe droughts for the SSP126 scenario is approximately the same as
666 in the past, but the duration will be substantially reduced. For scenarios SSP370 and SSP585, the number
667 of long-term severe droughts will increase more than during the historical period, but the duration will
668 be markedly less, and the deficit will be reduced to some extent. In terms of the different the sub-periods,
669 severe droughts in the upper NRB will be more severe during the near-future and end-century periods,
670 and relatively less severe in the mid-century period in comparison to the historical period. However,
671 overall, the droughts will be of shorter duration and characterized by an increased deficit under future
672 climates.

673



674

● Historical ● Near-future ● Mid-century ● End-century



675 Figure 9. Historical and projected duration-deficit relationship of each hydrological droughts at the Nenjiang
676 (the first row) and Dalai (the second row) Station. The historical period refers to 1971-2020 and the near-
677 future, mid-century and end-century refer to the 2026-2050, 2051-2075 and 2076-2100 under the
678 Socioeconomic Pathways (SSP) 126, SSP370 and SSP585 scenarios. The dark yellow lines in the horizontal
679 and vertical directions refer the 95% threshold lines for drought deficit and duration values, respectively. I,
680 II, III and IV refer to short-term light droughts, long-term light droughts, short-term severe droughts, and
681 long-term severe droughts, respectively.

682

683 Droughts brought about by future climate change at the Dalai Station located along the lower reaches
684 of the NRB will continue to be dominated by short-term slight droughts (Fig. 9d, 9e and 9f). For the
685 SSP126 scenario, the duration and deficit of the short-term slight droughts will be approximately the
686 same as those during historical times. However, the duration and deficit of short-term slight droughts
687 will increase given the conditions specified in the SSP370 and SSP585 scenarios. The duration of short-
688 term slight droughts will increase the most for scenario SSP370. In addition, under all three SSP
689 scenarios, long-term slight droughts will, in general, be reduced. In fact, under the SSP370 scenario,
690 long-term slight droughts will not occur. The number of short-term severe droughts will generally tend
691 to increase, with the most pronounced increase under the SSP585 scenario, followed by the SSP370
692 scenario. A slight increase will occur under the SSP126 scenario. However, long-term severe droughts
693 will increase substantially under the SSP126 and SSP370 scenarios. In particular, under the SSP370
694 scenario, the duration of long-term severe droughts will be exceptionally prolonged, and the severity
695 will be extraordinarily increased, indicating that the risk of droughts of long duration and with a severe
696 deficit will climb abnormally in some year. For example, under the conditions set by the SSP370
697 scenario, the deficit of long-term severe droughts will reach $-18,169 \text{ m}^3$ and $-18,457 \text{ m}^3$ during the near-
698 future and end-century periods. For the SSP585 scenario, long-term severe drought will occur only once
699 in the near-future, which is equivalent to the historical period. These results indicate that the risk of
700 future hydrologic droughts along the lower NRB will further increase even under the combined
701 influence of reservoirs and wetlands.



702

703 **4. Discussion**

704 4.1. Integrating wetlands and reservoir operation into basin hydrologic modeling and basin water 705 management

706 A series of studies have shown that the simulation and prediction of floods and droughts faces many
707 challenges, such as the scarcity of hydrometeorological driven data (Foulon et al., 2018), model errors
708 (Smakhtin, 2001; Staudinger et al., 2011; Golden et al., 2021) and anthropogenic disturbances (e.g.,
709 reservoir operation) (Brunner, 2021; Brunner et al., 2021). In this study, we developed a spatially
710 explicit hydrological model that considers wetland hydrological processes and reservoir operations
711 through coupling a distributed hydrological modeling platform with wetland modules and reservoir
712 simulation algorithms. We found that coupling wetland alone or coupling wetlands and reservoir with
713 hydrological model can improve model calibration results and model performance of capturing flood
714 and drought characteristics in a large river basin. Such model performance improvement can minimize
715 uncertainties (Zhao et al., 2016; Rajib et al., 2020b; Golden et al., 2021) and provide important
716 information for developing downstream water resources management. Previous studies have shown that
717 climate change is further exacerbating the risk of hydrological extremes, leading to an expanding of
718 flood and drought affected area (e.g., Hirabayashi et al., 2013; Diffenbaugh et al., 2015b; Wang et al.,
719 2021), which increase the complexity of accurate prediction and the challenge for effective mitigation.
720 Give that, projecting flood and drought risks in response to a changing climate requires robust
721 hydrologic models that take into account the important factors within a watershed that can largely
722 influence basin hydrological processes (Golden et al., 2021). Therefore, in basins that coexist with high-
723 coverage wetlands and multiple reservoirs, it is necessary to integrate wetlands and reservoir operation
724 into basin hydrological simulation, thus providing practical support for extreme hydrological risk
725 mitigation and water resource management under a changing climate.

726 4.2. Future flood and drought risks under the influences of upstream wetlands

727 We found that the risks of floods and droughts will overall increase in the upper NRB under future



728 climate change, even when considering flow regulation services provided by wetlands. The overall
729 increasing flood peak, flood volume and flashiness inform that future flood risk will be much higher
730 compared to the historical periods. In particular, the NRB may experience flood events with much longer
731 duration, extreme high peak flows, exceeding larger flood volumes and extraordinary strong flashiness
732 (Fig. Fig.4 a-d, Fig. 5 a-d and Table A1). These extreme floods may pose a greater risk than that caused
733 by the Great Flood of 1998 (a 100-year flood that resulted in huge losses in the NRB) during the
734 historical period. As an example, a flood events spanning 66 days with the peak flow of $16213 \text{ m}^3/\text{s}$ and
735 with the volume of $190 \times 10^8 \text{ m}^3$ will be happen during the end-century periods given the constraints of
736 the SSP-126 scenario (Fig.5 a-c). The increasing flood risks could be largely attribute to the increasing
737 precipitation extremes in the NRB under future climate change. As Wu et al.(2022) who predicted future
738 precipitation extremes and flood events and concluded that the increasing precipitation extremes will
739 bring about higher flood risks with the increase in warming levels. In addition, upstream wetlands may
740 aid in enhancing flood risks because wetlands in headwater areas generally tend to increase downstream
741 flood risks (Acreman and Holden, 2013; Wu et al., 2020; Acreman et al., 2021). Moreover, the
742 effectiveness of wetlands is probably limited to smaller flood and drought events (Vojinovic et al., 2021).
743 Therefore, upstream wetlands can't fully mitigate future flood risks under future climate change,
744 confirming that wetlands have limited potential to efficiently mitigate future climate change.

745 We also found that the duration of droughts would become longer and the number of drought days
746 per year will increase, accompanied by an increase in drought duration and drought deficit (Fig. 7, Fig.
747 8 and Table A2). Further, severe droughts in the upper NRB will be more severe under the SSP370 and
748 SSP585 scenarios. It is worth noting that the baseflow support function of the downstream wetlands
749 may help the reservoir to reduce drought risk to some extent (Min et al., 2010; Fossey and Rousseau,
750 2016; Ameli and Creed, 2019; Golden et al., 2021). However, when experiencing extreme droughts,
751 this baseflow support function of downstream wetlands remain minimal, this can be corroborated by the
752 substantial increase in long-term severe droughts at the Dalai Station. This is because the increased
753 evapotranspiration during extreme drought period can cause temporary water deficits in wetlands,
754 causing them to reduce low flows instead of supporting them (Bullock and Acreman, 2003; Golden et



755 al., 2016).

756 Headwater or upper wetlands remain an important part of the watershed landscape, and are often
757 important natural reserves that cannot be reconstructed and transformed in the same way as downstream
758 wetlands (Colvin et al., 2019; Acreman et al., 2021). Therefore, from perspective of NBS, their
759 implication in enhancing basin resilience to water hazards needs an extensively assessed. While
760 numerous studies have showed that flood and drought risks may increase in magnitude and frequency
761 (Roudier et al., 2016; Cook et al., 2020; Tabari et al., 2021), the projected results come with some degree
762 of uncertainty. However, this study further highlights that the amplifying effect of wetlands on flooding
763 cannot be ignored in the headwater areas or upper reaches of basins where wetlands are widely
764 distributed. It is therefore reasonable to argue that without consideration of wetlands can lead to very
765 different distinguished results from the actual ones, or even lead to poor decision making and probably
766 disaster occurrence.

767 4.3. The combining mitigation efficiency of wetlands and reservoir operation

768 The relative changes (compared with historical periods) of future flood and drought indices (Fig. 4
769 and Fig. 7), duration-peak flow-volume relationships (Fig. 6) and duration-deficit relationship (Fig. 9)
770 differ between the Nenjiang and Dalai stations under the same SSP scenario or in the same period,
771 indicating that reservoirs and downstream wetlands can modify the continuous propagation of upstream
772 flood and hydrological drought risks to the downstream. First, reservoirs and downstream wetlands can
773 help to reduce the risks of future floods and droughts to some extent, namely partially reduce flood peak
774 flow and flashiness, and decrease the number of droughts, annual drought days and drought deficit.
775 Second, reservoirs and downstream wetlands cannot completely eliminate flood and drought risks.
776 Because the flood duration and volume will overall increase at the Dalai station, especially that the
777 extreme floods will be more frequent in the future (Fig.6). Further, in addition to the number of droughts,
778 the percentage change values of the annual drought days, drought duration and deficit relative change
779 at the Dalai Station are greater than those of Nenjiang Station (Fig.8). This imply that the mitigation
780 effects on hydrological droughts is minimal. Such findings suggest that future climate change will lead
781 to an increase in the risk of hydrologic failure of existing basic grey (e.g., reservoir) and green (i.e.,



782 wetlands) infrastructures, thus posing large challenges for future socio-and eco-hydrological systems in
783 the downstream NRB.

784 4.4 Implications for flood and drought risk management under climate change

785 This modeling study predicts higher flood and drought risks in the NRB. This could impose a great
786 challenge to the operation of the Nierji Reservoir dam, i.e., to its effective operation for flood mitigation
787 and drought alleviation. To curb the flood and drought risks caused by future climate change in the NRB,
788 it is urgent to improve the water regulation capacity of the lower NRB. Although the Nierji Reservoir,
789 as previously argued, plays an important role in reducing floods and droughts, the potential for extreme
790 hydrological events in the future necessitate the application of various combinations of measures with
791 different scales of implementation (i.e., hybrid measures) (Vojinovic et al., 2021). However, compared
792 with the historical period, the existing wetlands in the NRB have been seriously degraded, such as the
793 weakening of the connectivity between riparian wetlands and the river channel, and the increased
794 fragmentation of wetlands, among other changes (Chen et al., 2021). These degraded wetlands cannot
795 play an effective role in mitigating floods and droughts under future climate change. Therefore, we insist
796 that the first remedial measure to be undertaken should be the implementation of wetland restoration
797 and protection projects, because studies have demonstrated that wetland coverage and their spatial
798 pattern can affect both basin physical conditions and human decision-making attitudes toward risk
799 (Zedler and Kercher, 2005; Javaheri and Babbar-Sebens, 2014; Martinez-Martinez et al., 2014; Gómez-
800 Baggethun et al., 2019). Given that the spatial location of wetlands within a river basin is also important
801 in determining the efficiency of their mitigation services (Zhang and Song, 2014; Gourevitch et al.,
802 2020; Li et al., 2021), optimization of wetland spatial patterns should be considered and can be carried
803 out to further enhance the role of wetlands in flood and drought defense.

804 In our view, the second important remedial measure that should be implemented is to improve the
805 existing reservoir operation schemes based on accurate hydrological forecasting. This requires, on one
806 hand, coupling of wetlands with hydrological processes and models to improve the simulation accuracy
807 of the upstream incoming water (i.e., runoff from the Nenjiang Station) to provide scientific support for
808 reservoir operation decisions. Concomitantly, it is necessary to modify the existing schemes for optimal



809 reservoir operation to improve the system's capacity to deal with extreme flood and drought risks.
810 Because the percentage increase in drought (Fig. 5) and flood indicators (Fig. 8) demonstrated that the
811 existing reservoir operation schemes are not effective in mitigating the risks associated with future
812 climate change-induced floods and droughts. Therefore, we need to re-examine and evaluate the flood
813 and drought risks in the NRB under future climate change and propose optimal operation schemes that
814 can maximize the reduction of flood and drought risks by the Nierji Reservoir. Traditionally, the water
815 level of a reservoir should be maintained at the designed flood limited water level during the flood
816 season, which does not consider river flow forecast. Ding et al.(2015) analyzed a concept that provides
817 a dynamic control of the maximum allowed water level during the flood season, for the Nierji Reservoir
818 dam. A reasonable approach to tackle this issue could be to considerate forecast uncertainty and
819 acceptable flood risk to minimize the total loss caused by flood and drought. Further modeling studies
820 with multi-objective optimization algorithm can help identify an optimum reservoir operation for best
821 economic and ecological outcomes.

822 4.5. Limitation and future work

823 Although our developed framework demonstrates good modeling results, uncertainties could exist in
824 the assessment. Aspects such as the accuracy and error of the input data (Lobligeois et al., 2014), the
825 choice of the objective function (Fowler et al., 2018), the length of the period considered during
826 calibration (Arsenault et al., 2018), and the model structure (Melsen et al., 2019) can all affect the
827 performance of a model to replicate streamflow, thus impacting flood and drought predictions of under
828 future climate change. For example, the resolution of the utilized DEM affects the determination of
829 wetland drainage watersheds and the wetland fill-spill processes (Grimm and Chu, 2020; Zeng et al.,
830 2020), which in turn affects the prediction of watershed-scale surface runoff and river flow. Although
831 we used relatively coarse resolution data (i.e., a 1 km resolution DEM and land-use cover data) and a
832 short calibration period (2011-2018), we clearly demonstrate that coupling wetlands and reservoirs are
833 amenable to runoff simulations of high accuracy and low uncertainty. In addition, due to a lack of
834 wetlands water balance monitoring data, this study only used river station data (which only considered
835 the cumulative hydrologic effect of upstream wetlands) for model calibration. As Driscoll et al.(2020)



836 and Evenson et al.(2018) reported that remotely sensed inundation data can help calibrate and verify
837 wetland-integrated into watershed models. Therefore, there are ongoing efforts to obtain sufficient data
838 on wetland area dynamics and evapotranspiration, water depth and volume, soil water content using
839 multi-source remote sensing data and actual observations to better calibrate/validate watershed
840 hydrological models, which are expected to further improve the model's capacity of capturing flood and
841 drought patterns. Further, the distance between the Nierji reservoir and the downstream Dalai station is
842 535.8 km. The confluence of tributaries in the river section between the reservoir and the Dalai
843 hydrological station can diminish the impacts of the reservoir on floods and droughts to some extent.
844 Therefore, a potential limitation or bias to mention in our work is that our results may potentially
845 underestimate the role of reservoir operation in conjunction with wetlands.

846 **5. Concluding remarks**

847 This study explored the integrative capability of wetlands and reservoir operations in mitigating
848 floods and hydrological droughts under future climate change. To achieve this, we developed a modeling
849 framework coupling wetlands and reservoir operations into a spatially-explicit hydrological model and
850 then applied it in a case study involving a 297,000-km² large river basin in northeast China. With this
851 framework we projected future floods and hydrological droughts under five future climate change
852 scenarios. We found that coupling wetlands and reservoir operations can slightly increase model
853 calibration results and efficiently improve model capacity to capture both flood and hydrological
854 drought characteristics in a river basin. The upper NRB will experience more severe flood and
855 hydrological droughts and can impose a great challenge to the effective operation of downstream
856 reservoir under the predicted future climate change scenarios. The risk of future floods and hydrologic
857 droughts along the lower NRB will further increase even under the combined influence of reservoirs
858 and wetlands. These results demonstrated that the risk of floods and droughts will overall increase
859 further under future climate change even under the combined influence of reservoirs and wetlands,
860 showing the urgency to implement wetland restoration and develop accurate forecasting systems. To
861 fully understand how wetland and reservoir operations may be influential and maintain an acceptable



862 level of risk, it is therefore necessary to consider an optimization of wetland spatial patterns and
863 reservoir operations simultaneously, thus achieving a collaborative optimization management to
864 maximum basin resilience to floods and hydrological droughts. Further, the effects of combining nature-
865 based solutions (e.g., wetlands) with traditional engineering solutions (e.g., reservoir) should both be
866 useful and necessary in the future for management decisions.

867

868

869

870 **Data Availability**

871 The data used in this study are openly available for research purposes. The five GCM outputs (GFDL-
872 ESM4, IPSL-CM6A-LR, MPI-ESM1-2-HR, MRI-ESM2-0, and UKESM1-0-L) used in this study are
873 publically available and were provided by the Inter-Sectoral Impact Model Intercomparison Project
874 (ISIMIP) (<https://esg.pik-potsdam.de/search/isimip/>). The CMhyd software is available at
875 <https://swat.tamu.edu/software/cmhyd>. The land-use/land-cover types, soil texture, and digital elevation
876 model for China can be downloaded from <https://www.resdc.cn/>. Data from the 88 weather stations
877 administered by National Meteorological Information Centre of China can be download at
878 <http://data.cma.cn>.

879

880

881



882 **Appendices:**

883 Table A1. Median values of historical (His) and projected flood characteristics (duration, peak flow, volume,
 884 and flashiness) at the Nenjiang and Dalai stations under different Socioeconomic Pathways (SSP) scenarios
 885 in the near-future (IV), mid-century (II) and end-century (III).

Duration	Peak flow			Volume			Flashiness					
	(m ³ /s)			(m ³)								
	SSP126	SSP370	SSP585	SSP126	SSP370	SSP585	SSP126	SSP370	SSP585	SSP126	SSP370	SSP585
<i>Nenjiang</i>												
His	14.5	14.5	14.5	2499.2	2499.2	2499.2	24.1	24.1	24.1	356.5	356.5	356.5
I	14	15	14	2697.8	3570.8	3872.6	21.8	29.34	26.9	571.6	575.5	382.4
II	18	13.5	14	4133.1	4326.5	3693.9	36.8	28.9	31.3	290.2	797.5	276.9
III	14	14	15	3724.8	3678.5	5525.6	27.1	30.3	29.9	588.5	633.7	793.2
<i>Dalai</i>												
His	15	15	15	4498.9	4498.9	4498.9	41.7	41.7	41.7	377	377.1	377.1
I	30	11	11	2661.3	4450.9	3925.2	50.3	32.6	32.3	251.3	513.1	527.7
II	16	13	12	4259.3	5111.1	4179.3	46.7	48.3	33.9	763	686.2	473.2
III	11.5	14.5	13	4171.8	5859.3	6762.5	30.4	48.3	48.1	781.4	605.1	990.4

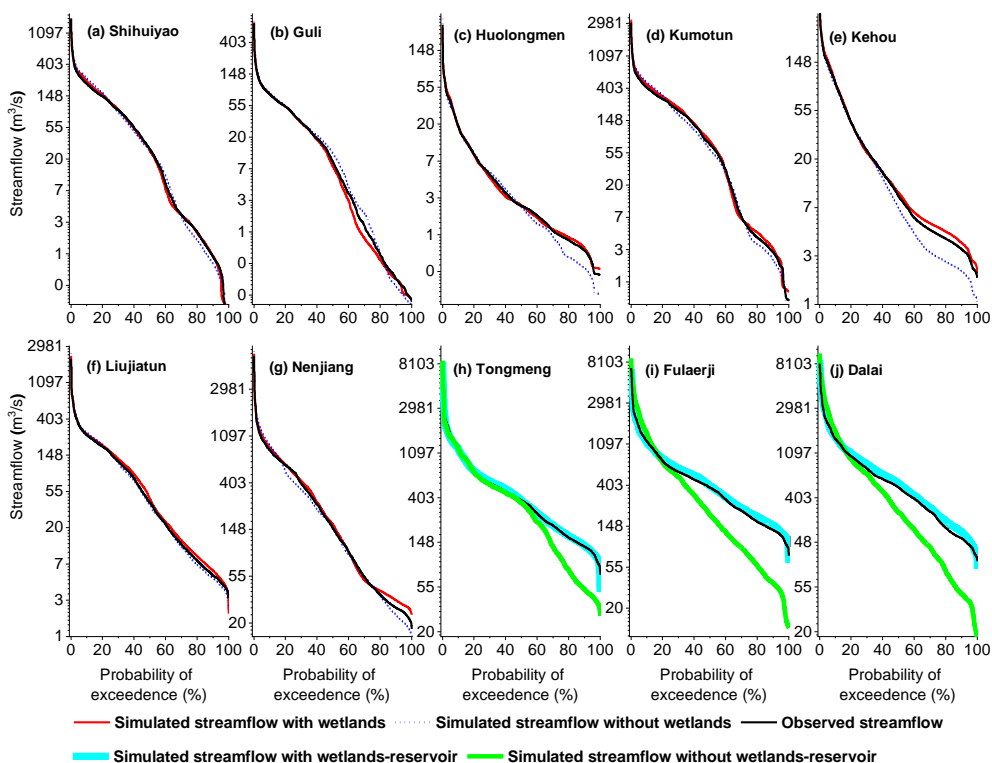
886



887 Table A2. Median values of historical (His) and projected of the projected number of droughts, annual
 888 drought days, duration, and deficit of each drought at the Nenjiang and Dalai stations under different
 889 Socioeconomic Pathways (SSP) scenarios in the near-future (I), mid-century (II) and end-century (III).

	Number of droughts			Annual drought days (days)			Drought duration (days)			Drought deficit (m ³)		
	SSP126	SSP370	SSP585	SSP126	SSP370	SSP585	SSP126	SSP370	SSP585	SSP126	SSP370	SSP585
<i>Nenjiang</i>												
His	2	2	2	20	20	20	10.5	10.5	10.5	-115.6	-115.6	-115.6
I	1	2	2	11	33	24	8	8	8	-136.8	-153.5	-163.3
II	4	2	3	58	38	29	9	9	10	-158.5	-159.8	-143.4
III	3.5	4	5	49	41	58	9	9	9	-186.7	-158.3	-164.6
<i>Dalai</i>												
His	2	2	2	15	15	15	8	8	8	-154.4	-154.4	-154.4
I	1	2	2	7	33	27	8	10	9	-337.6	-503.4	-449.1
II	3.5	2	2	57.5	19	20	11	10	10	-639.1	-360	-464
III	3	4	3	41	37	38	10	9	10	-629.1	-394.2	-591

890



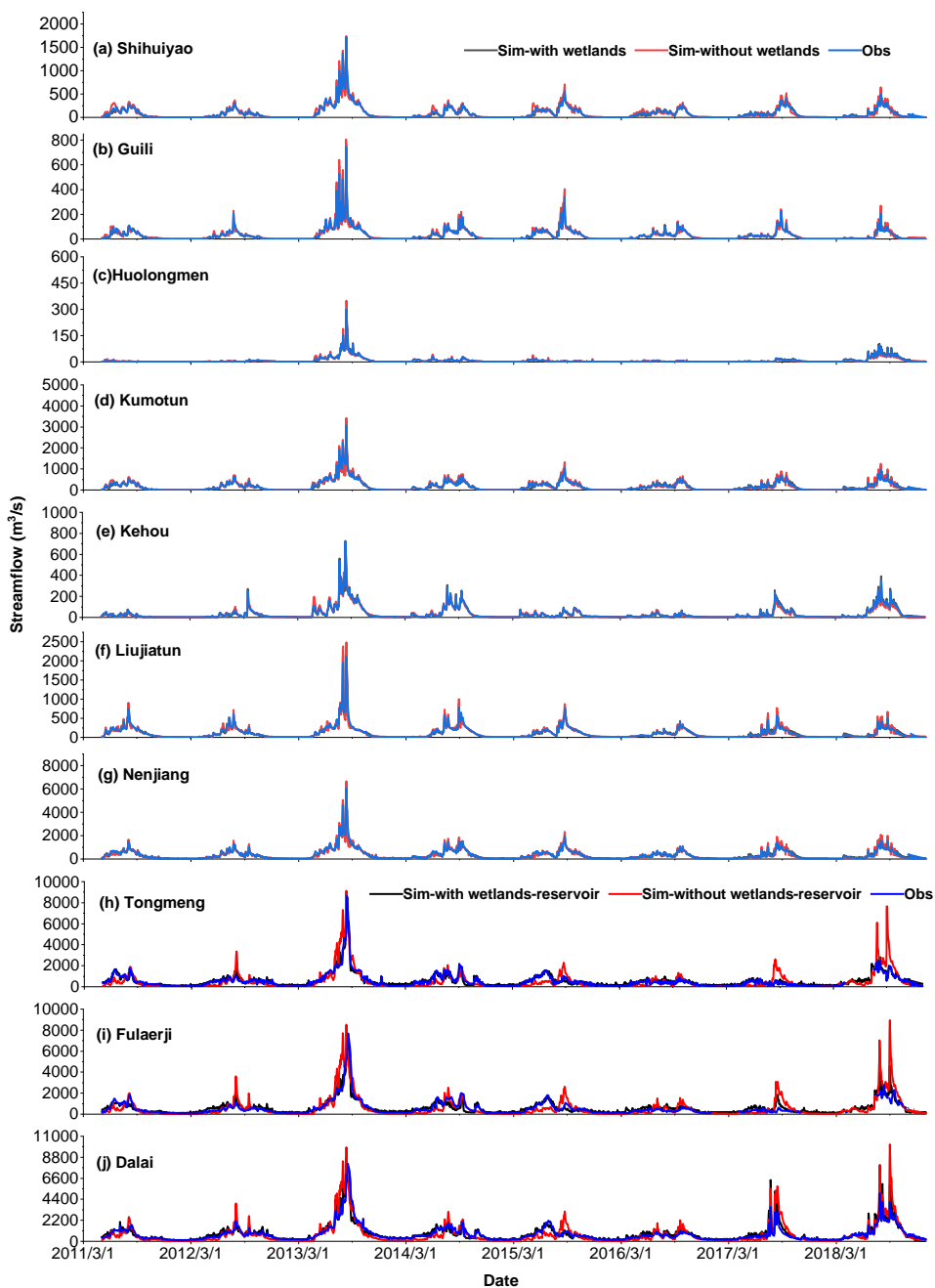
891

892 Fig. A1. Comparison of daily flow duration curves at ten hydrological stations in the Nenjiang River Basin.

893 The simulated streamflow used in Fig. 7a-g were calibrated with/without wetlands whereas the simulated

894 streamflow used in Fig. 7h-j were calibrated with/without wetlands and the Nierji reservoir.

895



896

897 Fig. A2. Comparison of daily simulated and observed streamflow at ten hydrological stations in the Nenjiang
898 River Basin. The simulated streamflow used in Fig. 6a-g were calibrated with/without wetlands whereas the
899 simulated streamflow used in Fig. 6h-j were calibrated with/without wetlands and the reservoir.

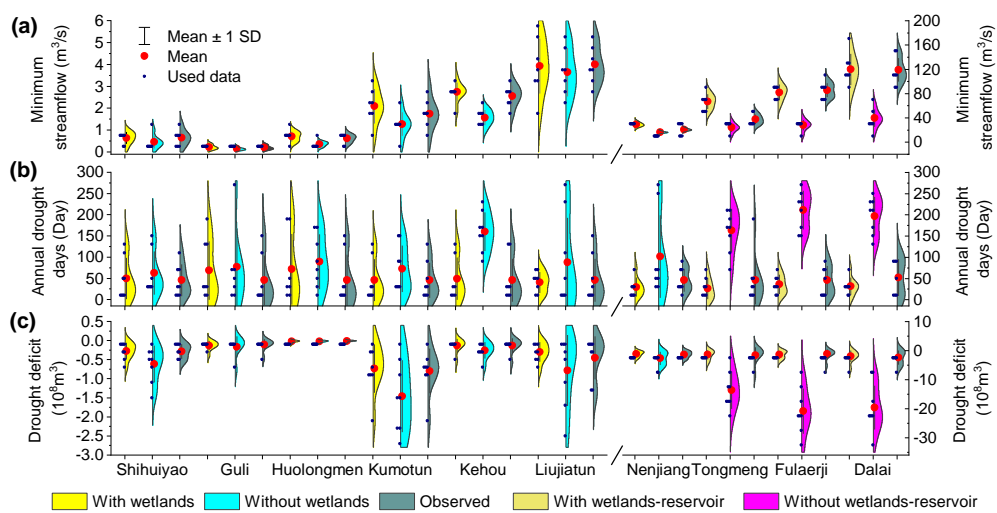
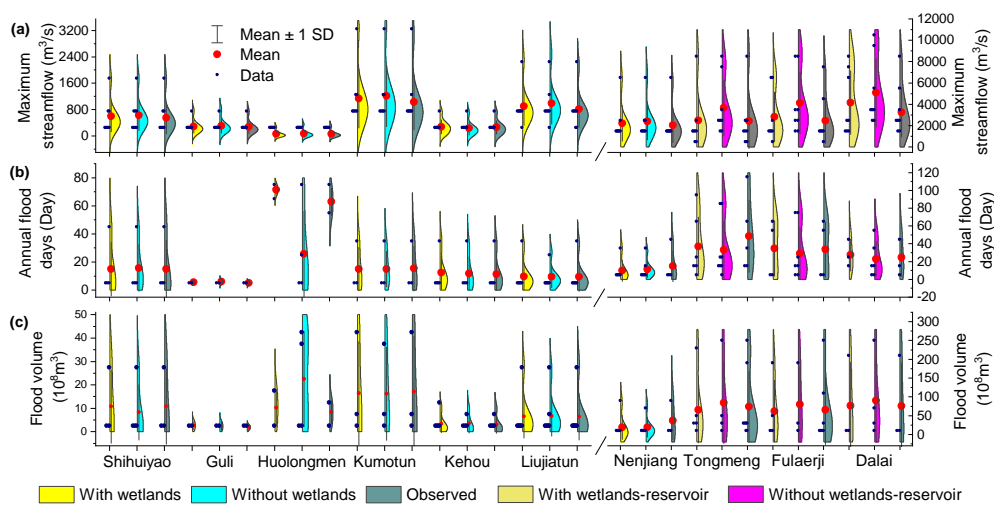


Fig. A3. Annual minimum streamflow, drought days and deficit derived from observed records and simulated streamflow at ten hydrological stations in the Nenjiang River Basin. The with and without wetlands/wetlands-reservoir refers to streamflow simulation based on the presence or absence of wetlands/wetlands and reservoir.



904

905

906

907

908

Fig. A4. Annual maximum peak flow, flood days and volume derived from observed records and simulated streamflow at ten hydrological stations in the Nenjiang River Basin. The with and without wetlands/wetlands-reservoir refers to streamflow simulation based on the presence or absence of wetlands/wetlands and reservoir.



909 **Author contribution**

910 **Yanfeng Wu:** Conceptualization, Writing, Data analysis, Methodology, Software. **Jingxuan Sun:**
911 Formal analysis, Investigation, Data analysis and Plotting. **Boting Hu:** Software, Visualization, Data
912 analysis. **Y. Jun Xu:** Writing - review & editing. **Alain N. Rousseau:** Writing - review & editing.
913 **Guangxin Zhang:** Conceptualization, Supervision, review & editing.

914

915 **Competing interests:**

916 The authors declare that they have no known competing financial interests or personal relationships
917 that could have appeared to influence the work reported in this paper.

918

919 **Acknowledgments**

920 This work was supported by the National Natural Science Foundation of China (42101051 and
921 41877160), the Postdoctoral Science Foundation of China (2021M693155), the Strategic Priority
922 Research Program of the Chinese Academy of Sciences, China (XDA28020501, XDA28020105), and
923 The National Key Research and Development Program of China (2021YFC3200203). During
924 preparation of this manuscript, YJX received a grant from U.S. Department of Agriculture Hatch Fund
925 (project number, LAB94459).

926

927

928 **References**

929 Acreman, M., Holden, J.: How Wetlands Affect Floods. *Wetlands* 33 (5), 773-786.
930 <https://doi.org/10.1007/s13157-013-0473-2>, 2013.
931 Acreman, M., Smith, A., Charters, L., Tickner, D., Opperman, J., Acreman, S., Edwards, F., Sayers,
932 P.Chivava, F.: Evidence for the effectiveness of nature-based solutions to water issues in Africa. *Environ.*
933 *Res. Lett.* 16 (6), 63007. <https://doi.org/10.1088/1748-9326/ac0210>, 2021.



- 934 Ahlén, I., Hambäck, P., Thorslund, J., Frampton, A., Destouni, G., Jarsjö, J.: Wetlandscape size thresholds for
935 ecosystem service delivery: Evidence from the Norrström drainage basin, Sweden. *Sci. Total Environ.*
936 704, 135452. <https://doi.org/10.1016/j.scitotenv.2019.135452>,2020.
- 937 Ahmed, F.: Cumulative Hydrologic Impact of Wetland Loss: Numerical Modeling Study of the Rideau River
938 Watershed, Canada. *J. Hydrol. Eng.* 19 (3), 593-606. [https://doi.org/10.1061/\(ASCE\)HE.1943-](https://doi.org/10.1061/(ASCE)HE.1943-5584.0000817)
939 5584.0000817,2014.
- 940 Alves, A., Gersonius, B., Kapelan, Z., Vojinovic, Z., Sanchez, A.: Assessing the Co-Benefits of green-blue-
941 grey infrastructure for sustainable urban flood risk management. *J. Environ. Manage.* 239, 244-254.
942 <https://doi.org/10.1016/j.jenvman.2019.03.036>,2019.
- 943 Ameli, A.A., Creed, I.F.: Does Wetland Location Matter When Managing Wetlands for Watershed - Scale
944 Flood and Drought Resilience? *JAWRA Journal of the American Water Resources Association* 55 (3),
945 529-542. <https://doi.org/10.1111/1752-1688.12737>,2019.
- 946 Anderson, C.C., Renaud, F.G.: A review of public acceptance of nature-based solutions: The ‘why’, ‘when’,
947 and ‘how’ of success for disaster risk reduction measures. *Ambio* 50 (8), 1552-1573,2021.
- 948 Arsenault, R., Brissette, F., Martel, J.: The hazards of split-sample validation in hydrological model calibration.
949 *J. Hydrol.* 566, 346-362. <https://doi.org/10.1016/j.jhydrol.2018.09.027>,2018.
- 950 Blanchette, M., Rousseau, A.N., Savary, S., Foulon, É.: Are spatial distribution and aggregation of wetlands
951 reliable indicators of stream flow mitigation? *J. Hydrol.* 608, 127646.
952 <https://doi.org/10.1016/j.jhydrol.2022.127646>,2022.
- 953 Bosshard, T., Kotlarski, S., Ewen, T., Schär, C.: Spectral representation of the annual cycle in the climate
954 change signal. *Hydrol. Earth Syst. Sci.* 15 (9), 2777-2788. [https://doi.org/10.5194/hess-15-2777-](https://doi.org/10.5194/hess-15-2777-2011)
955 2011,2011.
- 956 Bouda, M., Rousseau, A.N., Gumiere, S.J., Gagnon, P., Konan, B., Moussa, R.: Implementation of an
957 automatic calibration procedure for HYDROTEL based on prior OAT sensitivity and complementary
958 identifiability analysis. *Hydrol. Process.* 28 (12), 3947-3961,2014.
- 959 Bouda, M., Rousseau, A.N., Konan, B., Gagnon, P., Gumiere, S.J.: Bayesian Uncertainty Analysis of the
960 Distributed Hydrological Model HYDROTEL. *J. Hydrol. Eng.* 17 (9), 1021-1032.
961 [https://doi.org/10.1061/\(ASCE\)HE.1943-5584.0000550](https://doi.org/10.1061/(ASCE)HE.1943-5584.0000550),2012.



- 962 Boulange, J., Hanasaki, N., Yamazaki, D., Pokhrel, Y.: Role of dams in reducing global flood exposure under
963 climate change. *Nat. Commun.* 12 (1). <https://doi.org/10.1038/s41467-020-20704-0>, 2021.
- 964 Brunner, M.I.: Reservoir regulation affects droughts and floods at local and regional scales. *Environ. Res.
965 Lett.* 16 (12), 124016. <https://doi.org/10.1088/1748-9326/ac36f6>, 2021.
- 966 Brunner, M.I., Slater, L., Tallaksen, L.M., Clark, M.: Challenges in modeling and predicting floods and
967 droughts: A review. *Wiley Interdiscip. Rev.-Water* 8 (3). <https://doi.org/10.1002/wat2.1520>, 2021.
- 968 Bullock, A., Acreman, M.: The role of wetlands in the hydrological cycle. *Hydrol. Earth Syst. Sci.* 7 (3), 358-
969 389. <https://doi.org/10.5194/hess-7-358-2003>, 2003.
- 970 Cammalleri, C., Vogt, J., Salamon, P.: Development of an operational low-flow index for hydrological drought
971 monitoring over Europe. *Hydrological sciences journal* 62 (3), 346-358.
972 <https://doi.org/10.1080/02626667.2016.1240869>, 2017.
- 973 Casal-Campos, A., Fu, G., Butler, D., Moore, A.: An Integrated Environmental Assessment of Green and Gray
974 Infrastructure Strategies for Robust Decision Making. *Environ. Sci. Technol.* 49 (14), 8307-8314.
975 <https://doi.org/10.1021/es506144f>, 2015.
- 976 Chen, L., Wu, Y., Xu, Y., J. Guangxin, Z.: Alteration of flood pulses by damming the Nenjiang River, China
977 - Implication for the need to identify a hydrograph-based inundation threshold for protecting
978 floodplain wetlands. *Ecol. Indic.* 124, 107406. <https://doi.org/10.1016/j.ecolind.2021.107406>, 2021.
- 979 Chen, W., Nover, D., Yen, H., Xia, Y., He, B., Sun, W., Viers, J.: Exploring the multiscale hydrologic
980 regulation of multipond systems in a humid agricultural catchment. *Water Res.* 184, 115987.
981 <https://doi.org/https://doi.org/10.1016/j.watres.2020.115987>, 2020.
- 982 Cheng, C., Brabec, E., Yang, Y., Ryan, R., 2013. Rethinking stormwater management in a changing world:
983 Effects of detention for flooding hazard mitigation under climate change scenarios in the Charles River
984 Watershed, Proceedings of 2013 CELA Conference, Austin, Texas, pp. 27-30.
- 985 Chiang, F., Mazdiyasi, O., Aghakouchak, A.: Evidence of anthropogenic impacts on global drought
986 frequency, duration, and intensity. *Nat. Commun.* 12 (1). <https://doi.org/10.1038/s41467-021-22314-w>, 2021.
- 988 Colvin, S.A.R., Sullivan, S.M.P., Shirey, P.D., Colvin, R.W., Winemiller, K.O., Hughes, R.M., Fausch, K.D.,
989 Infante, D.M., Olden, J.D., Bestgen, K.R., Danehy, R.J., Eby, L.: Headwater Streams and Wetlands are



- 990 Critical for Sustaining Fish, Fisheries, and Ecosystem Services. *Fisheries* 44 (2), 73-91.
991 <https://doi.org/10.1002/fsh.10229,2019>.
- 992 Cook, B.I., Mankin, J.S., Marvel, K., Williams, A.P., Smerdon, J.E. Anchukaitis, K.J.: Twenty - First Century
993 Drought Projections in the CMIP6 Forcing Scenarios. *Earth's Future* 8 (6).
994 <https://doi.org/10.1029/2019EF001461,2020>.
- 995 Dang, T.D., Chowdhury, A.F.M.K. Galelli, S.: On the representation of water reservoir storage and operations
996 in large-scale hydrological models: implications on model parameterization and climate change impact
997 assessments. *Hydrol. Earth Syst. Sci.* 24 (1), 397-416. <https://doi.org/10.5194/hess-24-397-2020,2020>.
- 998 Diffenbaugh, N.S., Swain, D.L. Touma, D.: Anthropogenic warming has increased drought risk in California.
999 *Proceedings of the National Academy of Sciences* 112 (13), 3931-3936.
1000 <https://doi.org/10.1073/pnas.1422385112,2015a>.
- 1001 Diffenbaugh, N.S., Swain, D.L. Touma, D.: Anthropogenic warming has increased drought risk in California.
1002 *Proceedings of the National Academy of Sciences* 112 (13), 3931-3936.
1003 <https://doi.org/10.1073/pnas.1422385112,2015b>.
- 1004 Ding, W., Zhang, C., Peng, Y., Zeng, R., Zhou, H. Cai, X.: An analytical framework for flood water
1005 conservation considering forecast uncertainty and acceptable risk. *Water Resour. Res.* 51 (6), 4702-4726.
1006 <https://doi.org/10.1002/2015WR017127,2015>.
- 1007 Dobson, B., Wagener, T. Pianosi, F.: An argument-driven classification and comparison of reservoir operation
1008 optimization methods. *Adv. Water Resour.* 128, 74-86.
1009 <https://doi.org/10.1016/j.advwatres.2019.04.012,2019>.
- 1010 Driscoll, J.M., Hay, L.E., Vanderhoof, M.K. Viger, R.J.: Spatiotemporal Variability of Modeled Watershed
1011 Scale Surface - Depression Storage and Runoff for the Conterminous United States. *JAWRA Journal*
1012 *of the American Water Resources Association* 56 (1), 16-29. <https://doi.org/10.1111/1752-1688.12826,2020>.
- 1014 Eriyagama, N., Smakhtin, V. Udamura, L.: How much artificial surface storage is acceptable in a river basin
1015 and where should it be located: A review. *Earth-Sci. Rev.* 208, 103294.
1016 <https://doi.org/10.1016/j.earscirev.2020.103294,2020>.
- 1017 Evenson, G.R., Golden, H.E., Lane, C.R. D Amico, E.: Geographically isolated wetlands and watershed



- 1018 hydrology: A modified model analysis. *J. Hydrol.* 529, 240-256.
1019 <https://doi.org/10.1016/j.jhydrol.2015.07.039>,2015.
- 1020 Evenson, G.R., Golden, H.E., Lane, C.R.D'Amico, E.: An improved representation of geographically isolated
1021 wetlands in a watershed-scale hydrologic model. *Hydrol. Process.* 30 (22), 4168-4184.
1022 <https://doi.org/10.1002/hyp.10930>,2016.
- 1023 Evenson, G.R., Jones, C.N., Mclaughlin, D.L., Golden, H.E., Lane, C.R., Devries, B., Alexander, L.C., Lang,
1024 M.W., Mccarty, G.W.Sharifi, A.: A watershed-scale model for depressional wetland-rich landscapes. *J.*
1025 *Hydrol. X* 1, 100002. <https://doi.org/https://doi.org/10.1016/j.hydroa.2018.10.002>,2018.
- 1026 Fleig, A.K., Tallaksen, L.M., Hisdal, H.Demuth, S.: A global evaluation of streamflow drought
1027 characteristics. *Hydrol. Earth Syst. Sci.* 10 (4), 535-552. <https://doi.org/10.5194/hess-10-535-2006>,2006.
- 1028 Fortin, J., Turcotte, R., Massicotte, S., Moussa, R., Fitzback, J.Villeneuve, J.: Distributed Watershed Model
1029 Compatible with Remote Sensing and GIS Data. I: Description of Model. *J. Hydrol. Eng.* 6 (2), 91-99.
1030 [https://doi.org/10.1061/\(ASCE\)1084-0699\(2001\)6:2\(91\)](https://doi.org/10.1061/(ASCE)1084-0699(2001)6:2(91)),2001.
- 1031 Fossey, M.Rousseau, A.N.: Assessing the long-term hydrological services provided by wetlands under
1032 changing climate conditions: A case study approach of a Canadian watershed. *J. Hydrol.* 541, 1287-
1033 1302. <https://doi.org/https://doi.org/10.1016/j.jhydrol.2016.08.032>,2016.
- 1034 Fossey, M., Rousseau, A.N.Savary, S.: Assessment of the impact of spatio-temporal attributes of wetlands
1035 on stream flows using a hydrological modelling framework: a theoretical case study of a watershed
1036 under temperate climatic conditions. *Hydrol. Process.* 30 (11), 1768-1781.
1037 <https://doi.org/10.1002/hyp.10750>,2016.
- 1038 Fossey, M., Rousseau, A.N., Bensalma, F., Savary, S.Royer, A.: Integrating isolated and riparian wetland
1039 modules in the PHYSITEL/HYDROTEL modelling platform: model performance and diagnosis.
1040 *Hydrol. Process.* 29 (22), 4683-4702. <https://doi.org/https://doi.org/10.1002/hyp.10534>,2015.
- 1041 Foulon, É., Rousseau, A.N.Gagnon, P.: Development of a methodology to assess future trends in low flows
1042 at the watershed scale using solely climate data. *J. Hydrol.* 557, 774-790.
1043 <https://doi.org/10.1016/j.jhydrol.2017.12.064>,2018.
- 1044 Fowler, K., Peel, M., Western, A.Zhang, L.: Improved Rainfall - Runoff Calibration for Drying Climate:
1045 Choice of Objective Function. *Water Resour. Res.* 54 (5), 3392-3408.



- 1046 <https://doi.org/10.1029/2017WR022466>,2018.
- 1047 Fujimori, S., Hasegawa, T., Masui, T., Takahashi, K., Herran, D.S., Dai, H., Hijioka, Y., Kainuma, M.: SSP3:
1048 AIM implementation of Shared Socioeconomic Pathways. *Global Environmental Change* 42, 268-283.
1049 <https://doi.org/10.1016/j.gloenvcha.2016.06.009>,2017.
- 1050 Garcia, F., Folton, N., Oudin, L.: Which objective function to calibrate rainfall – runoff models for low-flow
1051 index simulations? *Hydrological Sciences Journal* 62 (7), 1149-1166.
1052 <https://doi.org/10.1080/02626667.2017.1308511>,2017.
- 1053 Golden, H.E., Lane, C.R., Rajib, A., Wu, Q.: Improving global flood and drought predictions: integrating non-
1054 floodplain wetlands into watershed hydrologic models. *Environ. Res. Lett.* 16 (9), 091002.
1055 <https://doi.org/10.1088/1748-9326/ac1fbc>,2021.
- 1056 Golden, H.E., Sander, H.A., Lane, C.R., Zhao, C., Price, K., D'Amico, E., Christensen, J.R.: Relative effects
1057 of geographically isolated wetlands on streamflow: a watershed-scale analysis. *Ecohydrology* 9 (1), 21-
1058 38. <https://doi.org/10.1002/eco.1608>,2016.
- 1059 Gómez-Baggethun, E., Tudor, M., Doroftei, M., Covaliov, S., Năstase, A., Onără, D., Mierlă, M., Marinov,
1060 M., Doroșencu, A., Lupu, G., Teodorof, L., Tudor, I., Köhler, B., Museth, J., Aronsen, E., Ivar Johnsen,
1061 S., Ibram, O., Marin, E., Crăciun, A., Cioacă, E.: Changes in ecosystem services from wetland loss and
1062 restoration: An ecosystem assessment of the Danube Delta (1960 – 2010). *Ecosyst. Serv.* 39, 100965.
1063 <https://doi.org/10.1016/j.ecoser.2019.100965>,2019.
- 1064 Gourevitch, J.D., Singh, N.K., Minot, J., Raub, K.B., Rizzo, D.M., Wemple, B.C., Ricketts, T.H.: Spatial
1065 targeting of floodplain restoration to equitably mitigate flood risk. *Global Environmental Change* 61,
1066 102050. <https://doi.org/10.1016/j.gloenvcha.2020.102050>,2020.
- 1067 Grimm, K.C., Chu, X.: Depression threshold control proxy to improve HEC-HMS modeling of depression-
1068 dominated watersheds. *Hydrological Sciences Journal* 65 (2), 200-211.
1069 <https://doi.org/10.1080/02626667.2019.1690148>,2020.
- 1070 Gulbin, S., Kirilenko, A.P., Kharel, G., Zhang, X.: Wetland loss impact on long term flood risks in a closed
1071 watershed. *Environ. Sci. Policy* 94, 112-122. <https://doi.org/10.1016/j.envsci.2018.12.032>,2019.
- 1072 Güneralp, B., Güneralp, O., Liu, Y.: Changing global patterns of urban exposure to flood and drought hazards.
1073 *Global Environmental Change* 31, 217-225. <https://doi.org/10.1016/j.gloenvcha.2015.01.002>,2015.



- 1074 Gupta, H.V., Kling, H., Yilmaz, K.K.Martinez, G.F.: Decomposition of the mean squared error and NSE
1075 performance criteria: Implications for improving hydrological modelling. *J. Hydrol.* 377 (1-2), 80-91.
1076 <https://doi.org/10.1016/j.jhydrol.2009.08.003>,2009.
- 1077 Hagemann, S.Jacob, D.: Gradient in the climate change signal of European discharge predicted by a multi-
1078 model ensemble. *Clim. Change* 81 (S1), 309-327. <https://doi.org/10.1007/s10584-006-9225-0>,2007.
- 1079 Hallegatte, S., Green, C., Nicholls, R.J.Coffee-Morlot, J.: Future flood losses in major coastal cities. *Nat.*
1080 *Clim. Chang.* 3 (9), 802-806,2013.
- 1081 Hirabayashi, Y., Mahendran, R., Koirala, S., Konoshima, L., Yamazaki, D., Watanabe, S., Kim, H.Kanae, S.:
1082 Global flood risk under climate change. *Nat. Clim. Chang.* 3 (9), 816-821.
1083 <https://doi.org/10.1038/nclimate1911>,2013.
- 1084 Hisdal, H.Tallaksen, L.M.: Estimation of regional meteorological and hydrological drought characteristics:
1085 a case study for Denmark. *J. Hydrol.* 281 (3), 230-247. [https://doi.org/https://doi.org/10.1016/S0022-1694\(03\)00233-6](https://doi.org/https://doi.org/10.1016/S0022-1694(03)00233-6),2003.
- 1087 Hutchinson, M.F.Xu, T.: Anusplin version 4.2 user guide. Centre for Resource and Environmental Studies.
1088 The Australian National University. Canberra 5,2004.
- 1089 Javaheri, A.Babbar-Sebens, M.: On comparison of peak flow reductions, flood inundation maps, and velocity
1090 maps in evaluating effects of restored wetlands on channel flooding. *Ecol. Eng.* 73, 132-145.
1091 <https://doi.org/10.1016/j.ecoleng.2014.09.021>,2014.
- 1092 Jongman, B.: Effective adaptation to rising flood risk. *Nat. Commun.* 9 (1), 1986.
1093 <https://doi.org/10.1038/s41467-018-04396-1>,2018.
- 1094 Kharrufa, N.S.: Simplified equation for evapotranspiration in arid regions. *Hydrologie Sonderheft* 5 (1), 39
1095 - 47,1985.
- 1096 Kriegler, E., Bauer, N., Popp, A., Humpenöder, F., Leimbach, M., Strefler, J., Baumstark, L., Bodirsky, B.L.,
1097 Hilaire, J., Klein, D., Mouratiadou, I., Weindl, I., Bertram, C., Dietrich, J., Luderer, G., Pehl, M.,
1098 Pietzcker, R., Piontek, F., Lotze-Campen, H., Biewald, A., Bonsch, M., Giannousakis, A., Kreidenweis,
1099 U., Müller, C., Rolinski, S., Schultes, A., Schwanitz, J., Stevanovic, M., Calvin, K., Emmerling, J.,
1100 Fujimori, S.Edenhofer, O.: Fossil-fueled development (SSP5): An energy and resource intensive
1101 scenario for the 21st century. *Global Environmental Change* 42, 297-315.



- 1102 <https://doi.org/https://doi.org/10.1016/j.gloenvcha.2016.05.015,2017>.
- 1103 Kumar, P., Debele, S.E., Sahani, J., Rawat, N., Marti-Cardona, B., Alfieri, S.M., Basu, B., Basu, A.S.,
1104 Bowyer, P., Charizopoulos, N., Gallotti, G., Jaakko, J., Leo, L.S., Loupis, M., Menenti, M., Mickovski,
1105 S.B., Mun, S.J., Gonzalez-Ollauri, A., Pfeiffer, J., Pilla, F., Proll, J., Rutzinger, M., Santo, M.A.,
1106 Sannigrahi, S., Spyrou, C., Tuomenvirta, H.Zieher, T.: Nature-based solutions efficiency evaluation
1107 against natural hazards: Modelling methods, advantages and limitations. *Sci. Total Environ.* 784,
1108 147058. <https://doi.org/10.1016/j.scitotenv.2021.147058,2021>.
- 1109 Lee, S., Yeo, I.Y., Lang, M.W., Sadeghi, A.M., Mccarty, G.W., Moglen, G.E.Evenson, G.R.: Assessing the
1110 cumulative impacts of geographically isolated wetlands on watershed hydrology using the SWAT model
1111 coupled with improved wetland modules. *J. Environ. Manage.* 223, 37-48.
1112 <https://doi.org/10.1016/j.jenvman.2018.06.006,2018>.
- 1113 Li, F., Zhang, G.Xu, Y.J.: Spatiotemporal variability of climate and streamflow in the Songhua River Basin,
1114 northeast China. *J. Hydrol.* 514, 53-64. <https://doi.org/10.1016/j.jhydrol.2014.04.010,2014>.
- 1115 Li, W., Jiang, Y., Duan, Y., Bai, J., Zhou, D.Ke, Y.: Where and how to restore wetland by utilizing storm
1116 water at the regional scale: A case study of Fangshan, China. *Ecol. Indic.* 122, 107246.
1117 <https://doi.org/https://doi.org/10.1016/j.ecolind.2020.107246,2021>.
- 1118 Liu, Y., Yang, W.Wang, X.: Development of a SWAT extension module to simulate riparian wetland
1119 hydrologic processes at a watershed scale. *Hydrol. Process.* 22 (16), 2901-2915.
1120 <https://doi.org/10.1002/hyp.6874,2008>.
- 1121 Lobligeois, F., Andréassian, V., Perrin, C., Tabary, P.Loumagne, C.: When does higher spatial resolution
1122 rainfall information improve streamflow simulation? An evaluation using 3620 flood events. *Hydrol.*
1123 *Earth Syst. Sci.* 18 (2), 575-594. <https://doi.org/10.5194/hess-18-575-2014,2014>.
- 1124 Maes, J., Barbosa, A., Baranzelli, C., Zulian, G., Batista E Silva, F., Vandecasteele, I., Hiederer, R., Lique,
1125 C., Paracchini, M.L., Mubareka, S., Jacobs-Crisioni, C., Castillo, C.P.Lavalle, C.: More green
1126 infrastructure is required to maintain ecosystem services under current trends in land-use change in
1127 Europe. *Landsc. Ecol.* 30 (3), 517-534. <https://doi.org/10.1007/s10980-014-0083-2,2015>.
- 1128 Manfreda, S., Miglino, D.Albertini, C.: Impact of detention dams on the probability distribution of floods.
1129 *Hydrol. Earth Syst. Sci.* 25 (7), 4231-4242. <https://doi.org/10.5194/hess-25-4231-2021,2021>.



- 1130 Maraun, D.: Bias Correcting Climate Change Simulations - a Critical Review. *Curr. Clim. Chang. Rep.* 2 (4),
1131 211-220. <https://doi.org/10.1007/s40641-016-0050-x>,2016.
- 1132 Martinez-Martinez, E., Nejadhashemi, A.P., Woznicki, S.A.Love, B.J.: Modeling the hydrological
1133 significance of wetland restoration scenarios. *J. Environ. Manage.* 133, 121-134.
1134 <https://doi.org/10.1016/j.jenvman.2013.11.046>,2014.
- 1135 Melsen, L.A., Teuling, A.J., Torfs, P.J.J.F., Zappa, M., Mizukami, N., Mendoza, P.A., Clark, M.P.Uijlenhoet,
1136 R.: Subjective modeling decisions can significantly impact the simulation of flood and drought events.
1137 *J. Hydrol.* 568, 1093-1104. <https://doi.org/10.1016/j.jhydrol.2018.11.046>,2019.
- 1138 Meng, B., Liu, J., Bao, K.Sun, B.: Water fluxes of Nenjiang River Basin with ecological network analysis:
1139 Conflict and coordination between agricultural development and wetland restoration. *J. Clean Prod.* 213,
1140 933-943. <https://doi.org/10.1016/j.jclepro.2018.12.243>,2019.
- 1141 Min, J., Perkins, D.B.Jawitz, J.W.: Wetland-Groundwater Interactions in Subtropical Depressional Wetlands.
1142 *Wetlands* 30 (5), 997-1006. <https://doi.org/10.1007/s13157-010-0043-9>,2010.
- 1143 Moore, K., Pierson, D., Pettersson, K., Schneiderman, E.Samuelsson, P.: Effects of warmer world scenarios
1144 on hydrologic inputs to Lake Mälaren, Sweden and implications for nutrient loads. *Hydrobiologia* 599
1145 (1), 191-199. <https://doi.org/10.1007/s10750-007-9197-8>,2008.
- 1146 Moriasi, D.N.: Model Evaluation Guidelines for Systematic Quantification of Accuracy in Watershed
1147 Simulations. *Trans. ASABE* 50 (3), 885-900. <https://doi.org/10.13031/2013.23153>,2007.
- 1148 Moriasi, D.N., Gitau, M.W., Pai, N.Daggupati, P.: Hydrologic and water quality models: Performance
1149 measures and evaluation criteria. *Trans. ASABE* 58 (6), 1763-1785,2015.
- 1150 Moriasi, D.N., Gitau, M.W., Pai, N.Daggupati, P.: Hydrologic and water quality models: Performance
1151 measures and evaluation criteria. *Trans. ASABE* 58 (6), 1763-1785.
1152 <https://doi.org/10.13031/trans.58.10715>,2015.
- 1153 Muller, M.: Hydropower dams can help mitigate the global warming impact of wetlands. *Nature* 566 (7744),
1154 315-317. <https://doi.org/10.1038/d41586-019-00616-w>,2019.
- 1155 N. Moriasi, D., G. Arnold, J., W. Van Liew, M., L. Bingner, R., D. Harmel, R.L. Veith, T.: Model Evaluation
1156 Guidelines for Systematic Quantification of Accuracy in Watershed Simulations. *Trans. ASABE* 50 (3),
1157 885-900. <https://doi.org/https://doi.org/10.13031/2013.23153>,2007.



- 1158 Nash, J.E.Sutcliffe, J.V.: River flow forecasting through conceptual models part I—A discussion of principles.
1159 J. Hydrol. 10 (3), 282-290,1970.
- 1160 Nelson, D.R., Bledsoe, B.P., Ferreira, S.Nibbelink, N.P.: Challenges to realizing the potential of nature-based
1161 solutions. Curr. Opin. Environ. Sustain. 45, 49-55.
1162 <https://doi.org/https://doi.org/10.1016/j.cosust.2020.09.001,2020>.
- 1163 Nika, C.E., Gusmaroli, L., Ghafourian, M., Atanasova, N., Buttiglieri, G.Katsou, E.: Nature-based solutions
1164 as enablers of circularity in water systems: A review on assessment methodologies, tools and indicators.
1165 Water Res. 183, 115988. <https://doi.org/https://doi.org/10.1016/j.watres.2020.115988,2020>.
- 1166 Noël, P., Rousseau, A.N., Paniconi, C.Nadeau, D.F.: Algorithm for delineating and extracting hillslopes and
1167 hillslope width functions from gridded elevation data. J. Hydrol. Eng. 19 (2), 366-374,2014.
- 1168 O'Neill, B.C., Tebaldi, C., van Vuuren, D.P., Eyring, V., Friedlingstein, P., Hurtt, G., Knutti, R., Kriegler, E.,
1169 Lamarque, J., Lowe, J., Meehl, G.A., Moss, R., Riahi, K.Sanderson, B.M.: The Scenario Model
1170 Intercomparison Project (ScenarioMIP) for CMIP6. Geosci. Model Dev. 9 (9), 3461-3482.
1171 <https://doi.org/10.5194/gmd-9-3461-2016,2016>.
- 1172 Pool, S., Vis, M., Seibert, J.Sveriges, L.: Evaluating model performance: towards a non-parametric variant
1173 of the Kling-Gupta efficiency. Hydrological sciences journal 63 (13-14), 1941-1953.
1174 <https://doi.org/10.1080/02626667.2018.1552002,2018>.
- 1175 Rajib, A., Golden, H.E., Lane, C.R.Wu, Q.: Surface Depression and Wetland Water Storage Improves Major
1176 River Basin Hydrologic Predictions. Water Resour. Res. 56 (7).
1177 <https://doi.org/10.1029/2019WR026561,2020a>.
- 1178 Rajib, A., Golden, H.E., Lane, C.R.Wu, Q.: Surface Depression and Wetland Water Storage Improves Major
1179 River Basin Hydrologic Predictions. Water Resour. Res. 56 (7), e2019WR026561.
1180 <https://doi.org/https://doi.org/10.1029/2019WR026561,2020b>.
- 1181 Roudier, P., Andersson, J.C.M., Donnelly, C., Feyen, L., Greuell, W.Ludwig, F.: Projections of future floods
1182 and hydrological droughts in Europe under a +2°C global warming. Clim. Change 135 (2), 341-355.
1183 <https://doi.org/10.1007/s10584-015-1570-4,2016>.
- 1184 Rousseau, A.N., Fortin, J., Turcotte, R., Royer, A., Savary, S., Quévy, F., Noël, P.Paniconi, C.: PHYSITEL,
1185 a specialized GIS for supporting the implementation of distributed hydrological models. Water News-



- 1186 Official Magazine of the Canadian Water Resources Association 31 (1), 18-20,2011.
- 1187 Saharia, M., Kirstetter, P., Vergara, H., Gourley, J.J., Hong, Y., Giroud, M.: Mapping Flash Flood Severity in
1188 the United States. *J. Hydrometeorol.* 18 (2), 397-411. <https://doi.org/10.1175/JHM-D-16-0082.1,2017>.
- 1189 Schneider, C., Flörke, M., De Stefano, L., Petersen-Perlman, J.D.: Hydrological threats to riparian wetlands
1190 of international importance – a global quantitative and qualitative analysis. *Hydrol. Earth Syst. Sci.*
1191 21 (6), 2799-2815. <https://doi.org/10.5194/hess-21-2799-2017,2017>.
- 1192 Seibert, J., Vis, M.J.P., Lewis, E., Meerveld, H.J.: Upper and lower benchmarks in hydrological modelling.
1193 *Hydrol. Process.* 32, 1120 - 1125,2018.
- 1194 Shafeeque, M., Luo, Y.: A multi-perspective approach for selecting CMIP6 scenarios to project climate change
1195 impacts on glacio-hydrology with a case study in Upper Indus river basin. *J. Hydrol.* 599, 126466.
1196 <https://doi.org/https://doi.org/10.1016/j.jhydrol.2021.126466,2021>.
- 1197 Shook, K., Papalexiou, S., Pomeroy, J.W.: Quantifying the effects of Prairie depressional storage complexes
1198 on drainage basin connectivity. *J. Hydrol.* 593, 125846.
1199 <https://doi.org/https://doi.org/10.1016/j.jhydrol.2020.125846,2021>.
- 1200 Smakhtin, V.U.: Low flow hydrology: a review. *J. Hydrol.* 240 (3), 147-186.
1201 [https://doi.org/https://doi.org/10.1016/S0022-1694\(00\)00340-1,2001](https://doi.org/https://doi.org/10.1016/S0022-1694(00)00340-1,2001).
- 1202 Staudinger, M., Stahl, K., Seibert, J., Clark, M.P., Tallaksen, L.M.: Comparison of hydrological model
1203 structures based on recession and low flow simulations. *Hydrol. Earth Syst. Sci.* 15 (11), 3447-3459.
1204 <https://doi.org/10.5194/hess-15-3447-2011,2011>.
- 1205 Tabari, H., Hosseinzadehtalaei, P., Thiery, W., Willems, P.: Amplified drought and flood risk under future
1206 socioeconomic and climatic change. *Earth's Future* 9 (10), e2021EF002295,2021.
- 1207 Tallaksen, L., Lanen, V.: Hydrological drought. Processes and estimation methods for streamflow and
1208 groundwater.,2004.
- 1209 Tallaksen, L.M., van Lanen, H.A.J.: Hydrological drought; processes and estimation methods for streamflow
1210 and groundwater. *Developments in water science* 48,2004.
- 1211 Thorslund, J., Jarsjo, J., Jaramillo, F., Jawitz, J.W., Manzoni, S., Basu, N.B., Chalov, S.R., Cohen, M.J.,
1212 Creed, I.F., Goldenberg, R., Hylén, A., Kalantari, Z., Koussis, A.D., Lyon, S.W., Mazi, K., Mard, J.,
1213 Persson, K., Pietro, J., Prieto, C., Quin, A., Van Meter, K., Destouni, G.: Wetlands as large-scale nature-



- 1214 based solutions: Status and challenges for research, engineering and management. *Ecol. Eng.* 108, 489-
1215 497. <https://doi.org/https://doi.org/10.1016/j.ecoleng.2017.07.012,2017>.
- 1216 Tolson, B.A., Shoemaker, C.A.: Dynamically dimensioned search algorithm for computationally efficient
1217 watershed model calibration. *Water Resour. Res.* 43 (1), 1-6, 2007.
- 1218 Turcotte, R., Fortin, L.G., Fortin, V., Fortin, J.P., Villeneuve, J.P.: Operational analysis of the spatial
1219 distribution and the temporal evolution of the snowpack water equivalent in southern Québec, Canada.
1220 *Hydrol. Res.* 38 (3), 211-234. <https://doi.org/10.2166/nh.2007.009,2007>.
- 1221 Unisdr, C.: *The human cost of natural disasters: A global perspective.*, 2015.
- 1222 van Vuuren, D.P., Riahi, K., Calvin, K., Dellink, R., Emmerling, J., Fujimori, S., Kc, S., Kriegler, E., Neill,
1223 B.O.: The Shared Socio-economic Pathways: Trajectories for human development and global
1224 environmental change. *Global Environmental Change* 42, 148-152.
1225 <https://doi.org/https://doi.org/10.1016/j.gloenvcha.2016.10.009,2017>.
- 1226 Vojinovic, Z., Alves, A., Gómez, J.P., Weesakul, S., Keerakamolchai, W., Meesuk, V., Sanchez, A.:
1227 Effectiveness of small- and large-scale Nature-Based Solutions for flood mitigation: The case of
1228 Ayutthaya, Thailand. *Sci. Total Environ.* 789, 147725.
1229 <https://doi.org/10.1016/j.scitotenv.2021.147725,2021>.
- 1230 Walz, Y., Janzen, S., Narvaez, L., Ortiz-Vargas, A., Woelki, J., Doswald, N., Sebesvari, Z.: Disaster-related
1231 losses of ecosystems and their services. Why and how do losses matter for disaster risk reduction? *Int.*
1232 *J. Disaster Risk Reduct.* 63, 102425. <https://doi.org/10.1016/j.ijdr.2021.102425,2021>.
- 1233 Wang, L., Chen, X., Shao, Q., Li, Y.: Flood indicators and their clustering features in Wujiang River, South
1234 China. *Ecol. Eng.* 76, 66-74. <https://doi.org/10.1016/j.ecoleng.2014.03.018,2015>.
- 1235 Wang, S., Zhang, L., She, D., Wang, G., Zhang, Q.: Future projections of flooding characteristics in the
1236 Lancang-Mekong River Basin under climate change. *J. Hydrol.* 602, 126778.
1237 <https://doi.org/10.1016/j.jhydrol.2021.126778,2021>.
- 1238 Wang, X., Yang, W., Melesse, A.M.: Using Hydrologic Equivalent Wetland Concept Within SWAT to
1239 Estimate Streamflow in Watersheds with Numerous Wetlands. *Trans. ASABE* 51 (1), 55-72.
1240 <https://doi.org/10.13031/2013.24227,2008>.
- 1241 Ward, P.J., de Ruiter, M.C., Mård, J., Schröter, K., Van Loon, A., Veldkamp, T., von Uexkull, N., Wanders,



- 1242 N., Aghakouchak, A., Arnbjerg-Nielsen, K., Capewell, L., Carmen Llasat, M., Day, R., Dewals, B., Di
1243 Baldassarre, G., Huning, L.S., Kreibich, H., Mazzoleni, M., Savelli, E., Teutschbein, C., van den Berg,
1244 H., van der Heijden, A., Vincken, J.M.R., Waterloo, M.J.Wens, M.: The need to integrate flood and
1245 drought disaster risk reduction strategies. *Water Security* 11, 100070.
1246 <https://doi.org/10.1016/j.wasec.2020.100070,2020>.
- 1247 Wu, Y., Sun, J., Jun Xu, Y., Zhang, G.Liu, T.: Projection of future hydrometeorological extremes and wetland
1248 flood mitigation services with different global warming levels: A case study in the Nenjiang river basin.
1249 *Ecol. Indic.* 140, 108987. <https://doi.org/10.1016/j.ecolind.2022.108987,2022>.
- 1250 Wu, Y., Zhang, G., Rousseau, A.N.Xu, Y.J.: Quantifying streamflow regulation services of wetlands with an
1251 emphasis on quickflow and baseflow responses in the Upper Nenjiang River Basin, Northeast China. *J.*
1252 *Hydrol.* 583, 124565. <https://doi.org/10.1016/j.jhydrol.2020.124565,2020>.
- 1253 Wu, Y., Zhang, G., Rousseau, A.N., Xu, Y.J.Foulon, É.: On how wetlands can provide flood resilience in a
1254 large river basin: A case study in Nenjiang river Basin, China. *J. Hydrol.* 587, 125012.
1255 <https://doi.org/10.1016/j.jhydrol.2020.125012,2020>.
- 1256 Wu, Y., Zhang, G., Xu, Y.J.Rousseau, A.N.: River Damming Reduces Wetland Function in Regulating Flow.
1257 *J. Water Resour. Plan. Manage.-ASCE* 147 (10). [https://doi.org/10.1061/\(ASCE\)WR.1943-5452.0001434,2021](https://doi.org/10.1061/(ASCE)WR.1943-5452.0001434,2021).
- 1259 Xu, X., Wang, Y., Kalcic, M., Muenich, R.L., Yang, Y.C.E.Scavia, D.: Evaluating the impact of climate
1260 change on fluvial flood risk in a mixed-use watershed. *Environ. Modell. Softw.* 122, 104031.
1261 <https://doi.org/10.1016/j.envsoft.2017.07.013,2019>.
- 1262 Yassin, F., Razavi, S., Elshamy, M., Davison, B., Sapriza-Azuri, G.Wheater, H.: Representation and
1263 improved parameterization of reservoir operation in hydrological and land-surface models. *Hydrol.*
1264 *Earth Syst. Sci.* 23 (9), 3735-3764. <https://doi.org/10.5194/hess-23-3735-2019,2019>.
- 1265 Zedler, J.B.Kercher, S.: WETLAND RESOURCES: Status, Trends, Ecosystem Services, and Restorability.
1266 *Annu. Rev. Environ. Resour* 30 (1), 39-74.
1267 <https://doi.org/10.1146/annurev.energy.30.050504.144248,2005>.
- 1268 Zelenhasić, E.Salvai, A.: A method of streamflow drought analysis. *Water Resour. Res.* 23 (1), 156-168,1987.
- 1269 Zeng, L., Shao, J.Chu, X.: Improved hydrologic modeling for depression-dominated areas. *J. Hydrol.* 590,



- 1270 125269. <https://doi.org/https://doi.org/10.1016/j.jhydrol.2020.125269,2020>.
- 1271 Zhang, X.Song, Y.: Optimization of wetland restoration siting and zoning in flood retention areas of river
1272 basins in China: A case study in Mengwa, Huaihe River Basin. *J. Hydrol.* 519, 80-93.
1273 <https://doi.org/10.1016/j.jhydrol.2014.06.043,2014>.
- 1274 Zhao, G., Gao, H., Naz, B.S., Kao, S.Voisin, N.: Integrating a reservoir regulation scheme into a spatially
1275 distributed hydrological model. *Adv. Water Resour.* 98, 16-31.
1276 <https://doi.org/10.1016/j.advwatres.2016.10.014,2016>.
- 1277 Zhao, Y., Dong, N., Li, Z., Zhang, W., Yang, M.Wang, H.: Future precipitation, hydrology and hydropower
1278 generation in the Yalong River Basin: Projections and analysis. *J. Hydrol.* 602, 126738.
1279 <https://doi.org/10.1016/j.jhydrol.2021.126738,2021>.
- 1280